University of Alberta

High Resolution Geophysical Survey over a Sweetgrass Dyke, Milk River, South Alberta

by

Wendell Pardasie

A thesis submitted to the Faculty of Graduate Studies and Research in partial fulfillment of the requirements for the degree of Master of Science

in

Geophysics

Department of Physics

Edmonton, Alberta

Fall 2003

National Library
of Canada

Acquisitions and
Bibliographic Services

395 Wellington Street
Ottawa ON K1A 0N4
Canada

Bibliothèque nationale
du Canada

Acquisisitons et
services bibliographiques

395, rue Wellington
Ottawa ON K1A 0N4
Canada

Your file Votre référence
ISBN: 0-612-87856-2
Our file Notre référence
ISBN: 0-612-87856-2

The author has granted a non-exclusive licence allowing the National Library of Canada to reproduce, loan, distribute or sell copies of this thesis in microform, paper or electronic formats.

The author retains ownership of the copyright in this thesis. Neither the thesis nor substantial extracts from it may be printed or otherwise reproduced without the author's permission.

L'auteur a accordé une licence non exclusive permettant à la Bibliothèque nationale du Canada de reproduire, prêter, distribuer ou vendre des copies de cette thèse sous la forme de microfiche/film, de reproduction sur papier ou sur format électronique.

L'auteur conserve la propriété du droit d'auteur qui protège cette thèse. Ni la thèse ni des extraits substantiels de celle-ci ne doivent être imprimés ou aturement reproduits sans son autorisation.

Canada

University of Alberta

Library Release Form

Name of Author:	Wendell Pardasie
Title of Thesis:	High Resolution Geophysical Survey over a Sweetgrass Dyke, Milk River, South Alberta
Degree:	Master of Science
Year this Degree Granted:	2003

Permission is hereby granted to the University of Alberta Library to reproduce single copies of this thesis and to lend or sell such copies for private, scholarly or scientific research purposes only.

The author reserves all other publication and other rights in association with the copyright in the thesis, and except as herein before provided, neither the thesis nor any substantial portion thereof may be printed or otherwise reproduced in any material form whatever without the author's prior written permission.

ilding,

September 23, 2003

University of Alberta

Faculty of Graduate Studies and Research

The undersigned certified that they have read, and recommend to the Faculty of Graduate Studies and Research for acceptance, a thesis entitled **High Resolution Geophysical Survey over a Sweetgrass Dyke, Milk River, South Alberta** submitted by **Wendell Pardasie** in partial fulfillment of the requirements for the degree of **Master of Science** in Geophysics.

Dr. O. Catuneanu

Date: 23/09/03

Abstract

Aeromagnetic surveys commissioned in the fall of 1992 illustrated the existence of long igneous dykes running from northern Montana to the southernmost part of Alberta. Over the last few years the Geophysics field school of the University of Alberta has carried out detailed ground magnetic and seismic surveys of some of these features. Therefore, the main focus of this study is to attempt to image the dykes and gain some insight into the general geology of the area.

The processed magnetic data shows two subparallel northwest trending anomalies. Forward modeling of a profile line intersecting these two anomalies illustrates two subparallel subvertical dykes to be the best fit where the width of the southernmost dyke increases from the bottom to the subsurface and the northernmost dyke regular in thickness. The processed seismic data does not show evidence of any such structures. However, diffractions in a raw shot traversing the anomalies show the presence of an obstacle, possibly the southernmost dyke.

To my daughter, Myca who was my main inspiration in writing this thesis.

Acknowledgements

I would like to recognize my wife, Jillian, for her tolerance, encouragement and dedication and for being my best friend. My parents, Nolan and Chandra and my brother, Rodney have been instrumental in most of my successes through out my life. I would like to thank them for their help and support. Without my family I would not be at this turning point in my life. In addition, I would like to acknowledge the Government of the Republic of Trinidad and Tobago for giving me the opportunity and the funding to pursue my MSc. in Geophysics.

I would like to thank Dr. Doug Schmitt for being my co-supervisor and finding a suitable project for me, as well as Dr. Moritz Heimpel for being my co-supervisor at such a late stage in my project and for his help in acquiring and processing the magnetic data. I would like to acknowledge Dr. Mauricio Sacchi for his unconditional interest in my project and his willingness to help, especially with the seismic portion of this thesis and Dr. Martyn Unsworth for his help and moral support.

I would like to thank Ms. Yajun Zhang for her tremendous help and guidance in processing the seismic data. Also, I would like to acknowledge Dr. Dean Rokosh for lending his invaluable expertise in the field of Geology to this project and Mr. Alex Walcott for helping in locating a well suited magnetic modeling package and sharing his knowledge. I would like to thank Uli Theune for his help in the technical editing of this thesis and for his regular inputs.

I would like to acknowledge my past and present colleagues Pavlo Cholach, Dr. Henning Kuehl, Michael Lazorek, Marko Mah, Cristina Moldoveanu-Constantinescu, Dr. Wolfgang Soyer and Marek Welz for their assistance and moral support.

I would like to thank Seismic Image Software Limited for providing the software for processing the seismic data.

Finally, I am especially gracious to the Almighty for his guidance and blessings.

Table of Contents

Chapter 1 – Introduction.....1

1.1 Background.....1

1.2 Thesis objectives.....4

1.3 Area of Study.....4

Chapter 2 – Geology of the Study Area.....6

2.1 Introduction.....6

2.2 Stratigraphy.....7

2.2.1 Precambrian Basement.....7

2.2.2 Western Canadian Sedimentary Basin.....11

2.2.3 Phanerozoic Stratigraphy.....13

2.3 Igneous Intrusions.....23

2.3.1 Sweetgrass Intrusives.....23

2.3.2 Sweetgrass Arc.....28

2.4 Summary.....29

Chapter 3 – Magnetic Data.....31

3.1 Introduction.....31

3.2 Background.....33

3.3 Acquisition.....37

3.4 Processing.....38

3.4.1 Methodology.....38

3.4.2 Results.....40

3.5 Modelling.....45

3.6 Summary.....50

Chapter 4 – Seismic Data.....52

4.1 Introduction.....52

4.2 Acquisition.....54

4.3 Processing.....55

4.3.1 Methodology.....55

4.3.2 Results.....61

4.4 Seismic Modelling and Interpretation 65

4.5 Seismic Resolution Issues.....69

4.6 Summary.....71

Chapter 5 - Discussion and Conclusion.....73

Bibliography.....78

List of Tables

Table 3.1: Position of the magnetic profile line relative to the central seismic line and the magnitudes of their anomalies.....43

Table 4.1: Interpreted formation tops and their 2 way travel time and depth.....68

List of Figures

Figure 1.1: Major divisions of the geological time scale 3

Figure 1.2: Location map showing the study area. Red line represents the seismic line coverage (~2.5km) and blue area the magnetic coverage (1.6km NS and 1.3km EW). The position of the tie well, B.A.HB Verdures 7-26-03-14W4 relative to the survey area is also shown..... 5

Figure 2.1: Bedrock map showing some important features such as the Canadian Shield, WCSB, Foothills and Rocky Mountains and the ages of their surface rocks. (Modified from McQueen, 1994)..... 8

Figure 2.2: The location map of the Alberta and Williston Basins in relation to the SGI and the Foreland Thrust and Belt. (Modified from the Geological Atlas of the WCSB, Mossop & Shetsen, Chapter 3, 1994)..... 9

Figure 2.3: Map of exposed and subsurface basement terranes of Alberta. The study area is in the Medicine Hat Block region. (Modified from Ross et. al., 1991 and detailed documentation by Villeneuve et. al., 1993) 10

Figure 2.4: Location map showing the Canadian Shield, WCSB, Rocky Mountains and study area (not to scale) within Alberta, Canada..... 12

Figure 2.5: West to East crossection illustrating the thinning Phanerozoic wedge of the 13

WCSB. (Modified from the Geological Atlas of the WCSB, Mossop & Shetsen, Chapter 3, 1994) 13

Figure 2.6: Stratigraphic column for southern Alberta up to the first formation below the surface casing. (Modified from Meyboom, 1960). 14

Figure 2.7: The Stratigraphic chart for the B.A. HB Verdigris well log approximately 1.2km NE of the study area. Formations from below the surface casing to the Cambrian Period 17

Figure 2.8: Location map for northwestern United States showing the SGI (red star in dotted box), Sweetgrass Hills (red circle in dotted box) in the Montana alkaline igneous province, the Archean Wyoming cratonic block and GFTZ. (Modified from Buhlmann et. al., 2000) 24

Figure 2.9: Location map showing the SGI in the Milk River area, southern Alberta, as well as, the Sweetgrass Hills in Montana. The SGI is approximately 12km southeast of the study area. (Modified from Kjarsgaard, 1994) 25

Figure 3.1: The University of Alberta GSM-19 Overhauser Proton Precession Magnetometer. 32

Figure 3.2: A location map showing the Cypress Hills survey area in southern Alberta where the GSC collected aeromagnetic data in the fall of 1992. The stars in the Alberta region are termed the Sweetgrass Intrusives (Kjarsgaard, 1994). Figure modified from Ross et. al., 1996 34

Figure 3.3: Total Intensity map for the Cypress Hills survey area. The International Geomagnetic Reference Field was removed for an altitude of 1.1km. Figure modified from Ross et. al., 1996 35

Figure 3.4: First vertical derivative of the total intensity aeromagnetic data. Figure modified from Ross et. al., 1996. 35

Figure 3.5: Processing flow for the magnetic data set. 39

Figure 3.6 (a) to (h): Plot of the magnetic field (nT) versus profile lines south to North (left to right). The blue curve represents the diurnally corrected data and the red the low pass filtered data. (a) has vertical scale 1cm=100nT, (b) to (h) is 1cm=20nT. Horizontal scale is 1cm=300m. 41

Figure 3.6 (i) to (o): Plot of the magnetic field (nT) versus profile lines south to North (left to right). The blue curve represents the diurnally corrected data and the red the low pass filtered data. (i) to (m) is 1cm=20nT and (n) to (o) is 1cm=8nT. Horizontal scale is 1cm=300m. 42

Figure 3.7: Image of processed magnetic data together with the seismic reflection survey coverage (central bold line, i.e., 8th profile line to the left). Vertical and horizontal scales is 1cm=200m 45

Figure 3.8: The blue line represents the observed data and the red the modeled data. Top graph is total magnetic field intensity, TMI (nT) vs. offset, P(m) and bottom graph is depth, z (m) vs. northings, Y(m). Larger southerly dyke (red): width=10m, k=0.025. The other dyke (black): width=5m, k=0.02. In both cases Z=-70m, strike and dip are N124°E and 63°SW respectively. 47

Figure 3.9: The blue line represents the observed data and the red the modeled data. Top graph is total magnetic field intensity, TMI (nT) vs. offset, P(m) and bottom graph is depth, z (m) vs. northings, Y(m). The southerly dyke, Z=-80m, width and k of red portion is 4m and 0.025 and width and k of the green portion is 20m and 0.02 respectively. The other dyke (black): z=-65m, width=5m and k=0.02. In both cases, strike and dip are N124°E and 63°SW respectively. 48

Figure 3.10: The blue line represents the observed data and the red the modeled data. Top graph is total magnetic field intensity, TMI (nT) vs. offset, P(m) and bottom graph is depth, z (m) vs. northings, Y(m). The southerly dyke, Z=-85m, width and k of red portion is 4m and 0.015 and width and k of the green portion is 20m and 0.02 respectively. The other dyke (black): z=-65m, width=5m and k=0.02. In both cases, strike and dip are N124°E and 63°SW respectively..... 49

Figure 4.1: The University of Alberta's 2000-6000lbs vibroseis. The top left corner shows a geophone and a geode "box" below..... 53

Figure 4.2: Processing flow for the Milk River reflection seismic data set. Modified from Yilmaz, 1987..... 57

Figure 4.3: Shot gather for the northernmost shot point (shot 101 from the Milk River data set). Top horizontal axis is Shot point # (Sh Pt #), channel number (Ch #) – scale 3cm=50Ch and northings (N) in metres – scale 3cm=200m. Vertical axis is time in milliseconds – 1cm=300ms. Top figure shows a raw shot (Shot 101 from the Milk River data set) and bottom figure shows the raw shot after applying an AGC scaling and a band pass filter..... 59

Figure 4.4: Processed seismic data in VISTA using process flow from Figure 4.2. Top horizontal axis is common midpoint number (CMP #) – scale 3cm=50CMP and northings (N) in metres – scale 3cm=400m. Vertical axis is time in milliseconds – 1cm=200ms. Bottom graph (red) shows the magnetic profile along the seismic line, magnetic field (nT) vs. N (m) - Vertical scale 1cm=40nT and horizontal scale 3cm=400m 61

Figure 4.5: Shot gather for the northernmost shot point (shot 101 from the Milk River data set). Top horizontal axis is Shot point # (Sh Pt), channel number (Ch #) – scale 3cm=50Ch and northings (N) in metres – scale 3cm=200m. Vertical axis is time in milliseconds – 1cm=250ms. Bottom graph (red) shows the magnetic profile along the seismic line, magnetic field (nT) vs. N (m) - Vertical scale 1cm=40nT and horizontal scale 3cm=400m..... 63

Figure 4.6: Shot gather for the shot point 401, approximately 1.2km south of northernmost shot point. Top horizontal axis is Shot point (Sh Pt), channel number (Ch #) – scale 3cm=50Ch and northings (N) in metres – scale 3cm=200m. Vertical axis is time in milliseconds – 1cm=200ms. Bottom graph (red) shows the magnetic profile along the seismic line, magnetic field (nT) vs. N (m) - Vertical scale 1cm=40nT and horizontal scale 3cm=400m..... 64

Figure 4.7: Time (s) versus depth (m) curve obtained from the well B.A.HB Verdigris (07-26-03-14W4). The formation tops encountered at this well; 2nd White Specks, Base of Fish Scales, Mannville, Sunburst, Reirdon, Livingstone, Banff, Exshaw, Stettler, Cooking Lake, Beaver Hill Lake, Deadwood, Pika, Eldon, Earlie, Cathedral and Mount Whyte are shown. 66

Figure 4.8: The interpreted seismic section using B.A.HB Verdigris well (red). Top horizontal axis is common midpoint number (CMP) – scale 3cm=20CMP. Vertical axis is time in seconds – 1cm=0.3s. Formation tops such as the Mannville (MNVL), Rierdon/Livingstone (R/Liv.), Stettler (Stet.), Beaver Hill Lake (BHL), Deadwood (DDWD), Pika and the Precambrian basement (PreC.) are shown. 67

Chapter 1

Introduction

1.1 Background

High-resolution aeromagnetic surveys commissioned in the fall of 1992 by the Geological Survey of Canada (GSC) over the Cypress Hills area in southern Alberta illustrated the existence of long igneous dykes running from northern Montana to the southernmost region of Alberta (Ross et. al, 1996). This 1992 data set (referred to as the Cypress Hills Survey area) confirmed the presence of basement sourced magnetic anomalies that were seen in a previous survey conducted in the 1960s (Ross et. al, 1996). In addition, the 1992 data set showed the presence of unusually high wavenumber anomalies within the sedimentary strata. Ross et. al, 1996, modeled and speculated as to origin of these anomalies.

This work provided the main motivation in undertaking this project. In addition, past ground magnetic surveys carried out by the field school classes showed the presence of magnetic anomalies, which could be interpreted as hypabyssal intrusives related to the nearby Sweetgrass Intusives (SGI).

Consequently, the University of Alberta Field School classes conducted magnetic and seismic surveys using the University's GSM-19 Overhauser Proton Precession Magnetometer and 2000-6000lb load Vibroseis respectively. In addition GPS x (East-West direction), y (North-South direction) and z (elevation) positions according to the Universal Transverse Mercator (UTM) Grid System were obtained using the University of Alberta's Trimble 4600 LS Differential GPS unit. The main focus of this thesis is to attempt to image these dykes and gain some insight into the geology of the survey area. Figure 1.1 shows the major divisions of the geological time scale, which is a necessary reference for Chapter 2 where the geology of Alberta and the study area are discussed.

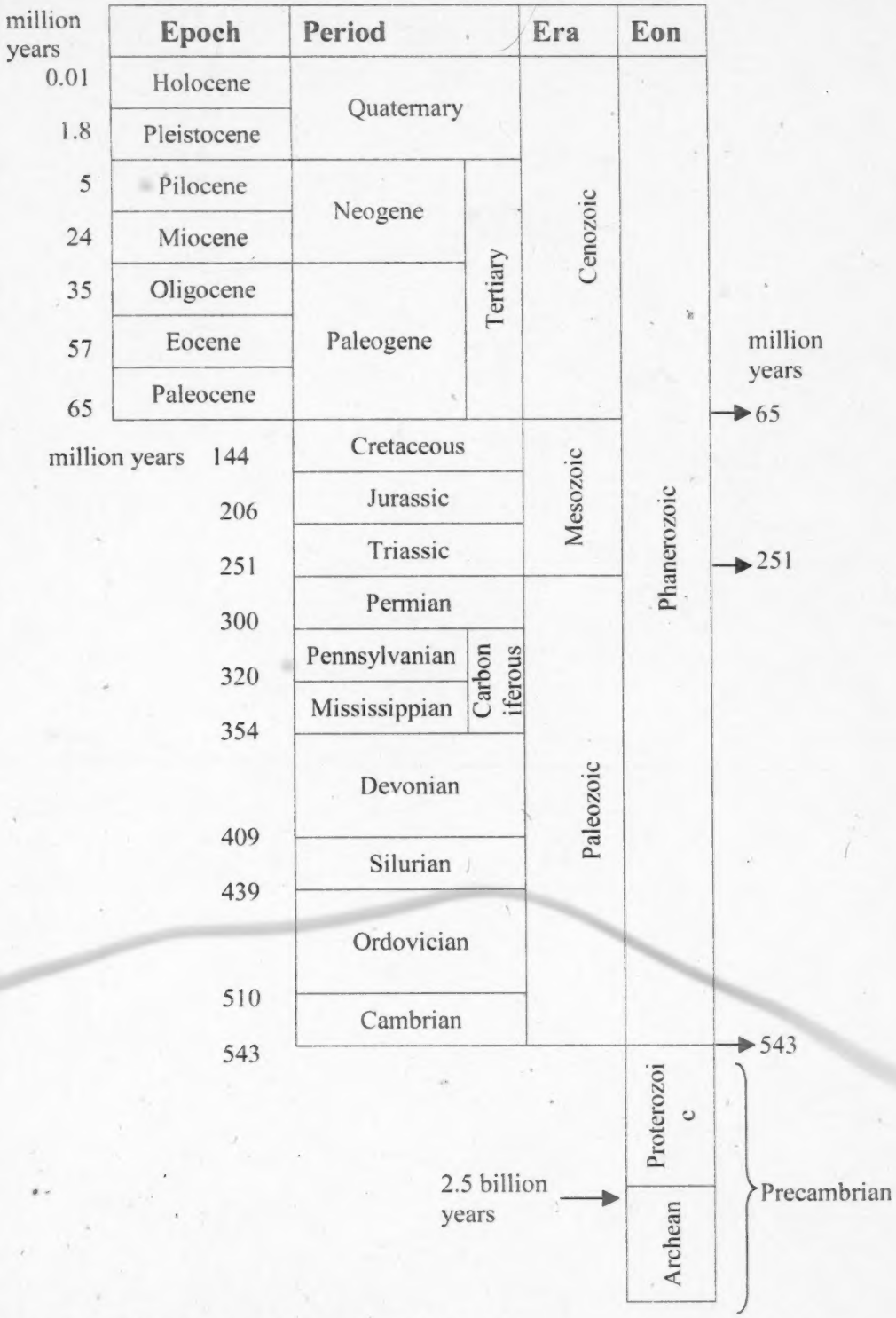

Figure 1.1: Major divisions of the geological time scale

1.2 Thesis Objectives

This thesis provides an overview of the data acquisition, processing and modelling and interpretation of magnetic and seismic data collected by the Field School classes of the University of Alberta near the Milk River area, Southern Alberta. In addition, a brief geological overview of Alberta and a more detailed geological study of the areas where the magnetic and seismic surveys were performed are incorporated.

1.3 Area of Study

The survey area shown in Figure 1.2 is located within 23-03-14W4 and 24-03-14W4 or in UTM coordinates, Zone U12 5450963-5453504m Northings and 443418-443449m Eastings. The red line represents the reflection seismic line, which has coverage of approximately 2.5km. Surrounding the seismic line is the blue area, which represents magnetic survey coverage. The magnetic survey area is approximately 1.6km in the north-south (NS) direction and 1.3km in the east-west direction (EW). Approximately, 1.2km northeast of the survey area is the tie well; B.A.HB Verdigris located 7-26-03-14W4, which was used for modelling and interpretation of the reflection seismic data.

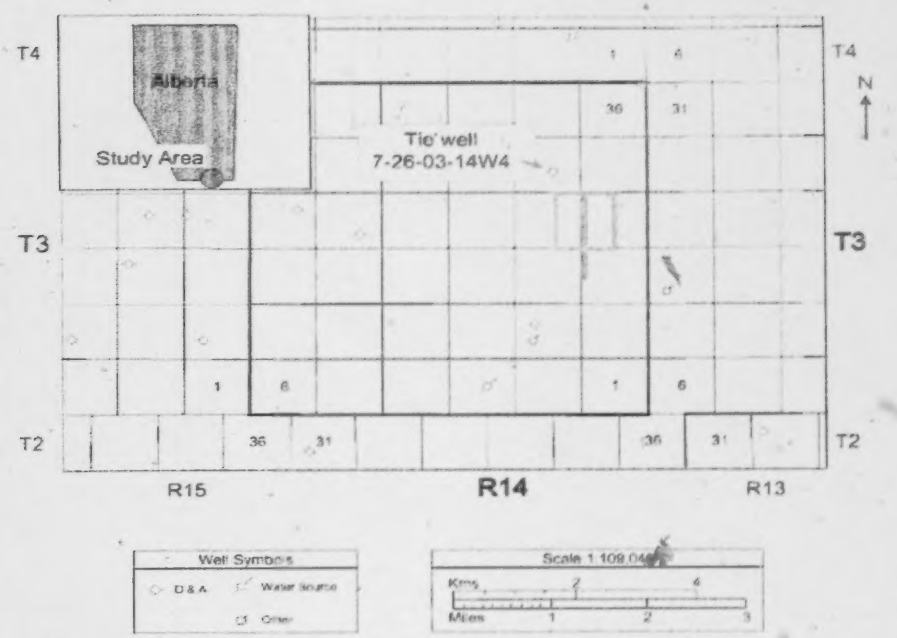

Figure 1.2: Location map showing the study area. Red line represents the seismic line coverage (~2.5km) and blue area the magnetic coverage (1.6km NS and 1.3km EW). The position of the tie well, B.A.HB Verdures 7-26-03-14W4 relative to the survey area is also shown.

Chapter 2

Geology of the Study Area

2.1 Introduction

Regionally, a brief description of the Western Canadian Sedimentary Basin (WCSB) together with the Precambrian (see Figure 1.1 in Chapter 1 which shows the major divisions of the geological time scale) basement is quite relevant, since our area of geophysical investigation is contained within it. Subsequently, focusing into the study area, the Phanerozoic stratigraphy is included in order to gain some insight on some of the existing formations. The Phanerozoic stratigraphy is based on geological data from Meyboon, 1960 (Figure 2.6) and a stratigraphic chart (Figure 2.7) derived from a tie well, B.A.HB Verdigris (07-26-03-14W4), which is approximately 1.2km northeast of the study area (Figure 1.2,

Chapter 1). The Geological Atlas of the Western Canadian Sedimentary Basin (Mossop & Shetsen, 1994) was the main source of information for the lithology of the study area, which was included in the Phanerozoic stratigraphy. Finally, the Sweetgrass Hills Intrusives (SGI), which are considered to be subordinate intrusions of the Sweetgrass Hills (Kjarsgaard, 1994) are both discussed in some detail. The Sweetgrass Hills and the SGI are of prime importance due to their characteristic dykes/plugs and, by correlation, are similar to features in the study area, which is approximately 12km northwest of the SGI.

2.2 Stratigraphy

2.2.1 Precambrian Basement

Alberta consists of portions of the three main geological provinces - the Canadian Shield, the Rocky Mountains and Foothills, and the WCSB (see Section 2.2.2). The Canadian Shield is in the northeast, the Rocky Mountains and Foothills in the southwest and the WCSB is between the Canadian Shield and the Rocky Mountains/Foothills and covers most of the province (Figure 2.1). The Rocky Mountains are comprised mostly of Paleozoic and Precambrian rocks and the Foothills contain Mesozoic subsurface rocks. The WCSB contains Tertiary rocks at the surface in the thicker area closer to the Foothills whereas in the shallower

region to the northeast Mesozoic rocks exist. Further to northeast corner of Alberta, Paleozoic rocks are present which merge with the Precambrian Canadian Shield.

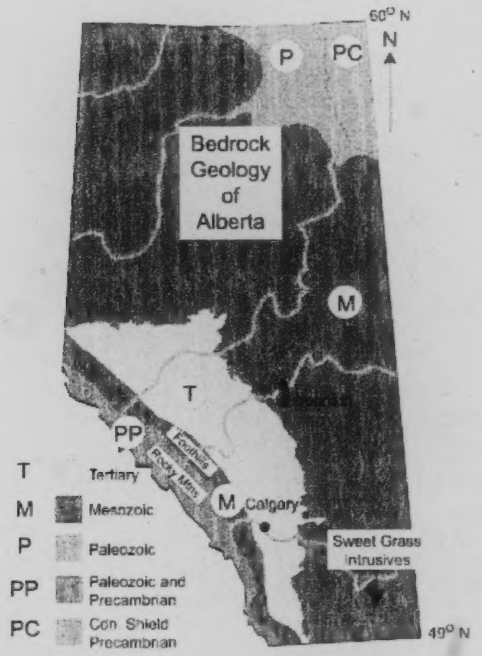

Figure 2.1: Bedrock map showing some important features such as the Canadian Shield, WCSB, Foothills and Rocky Mountains and the ages of their surface rocks. (Modified from McQueen, 1994)

The Alberta Basin (sometimes referred to as the Alberta Syncline) in the North and the Williston Basin in the South comprise part of the WCSB (Figure 2.2). The Alberta Basin is a northwest trending trough at the front of the Cordilleran Fold and Thrust Belt and extends eastward to the Canadian Shield. The Williston Basin is a cratonic basin centered in North Dakota and extends into southwest Manitoba and south Saskatchewan.

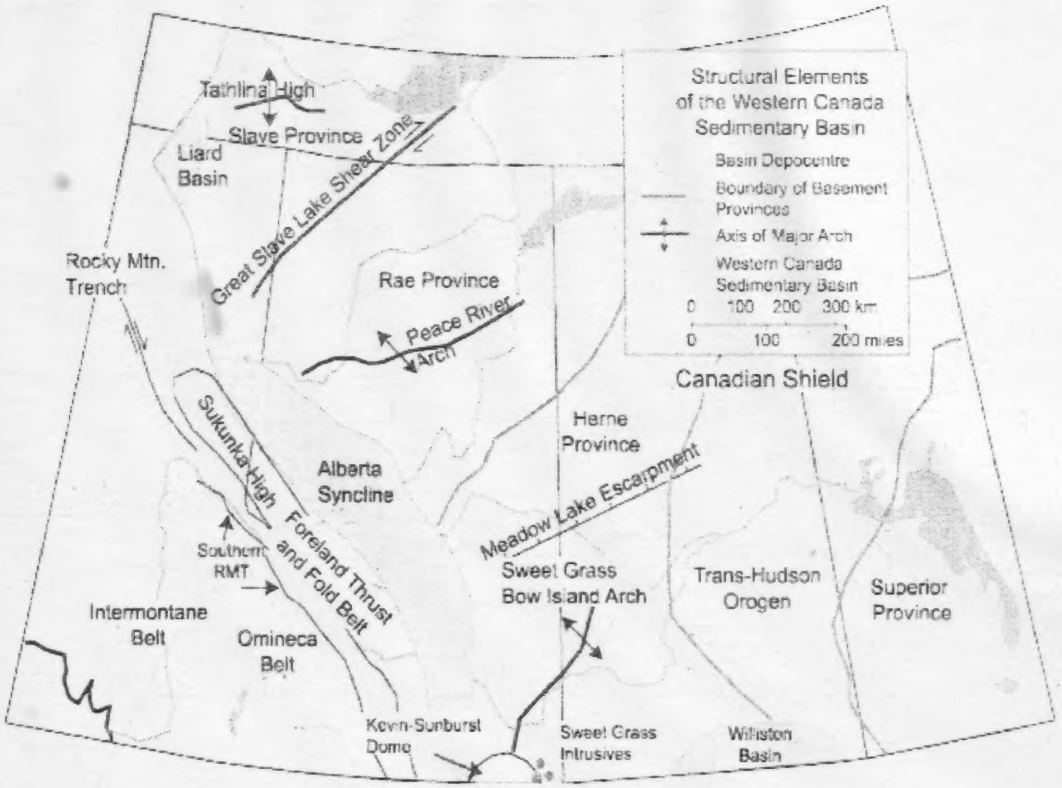

Figure 2.2: The location map of the Alberta and Williston Basins in relation to the SGI and the Foreland Thrust and Belt. (Modified from the Geological Atlas of the WCSB, Mossop & Shetsen, Chapter 3, 1994)

Since the WCSB rests on the Canadian Shield it is imperative that the basement rocks are described. The Canadian Shield is the large area of Precambrian rock that covers most of North America; that is, it extends from the North Eastern stable interior of North America; westward to the eastern Cordillera. In Alberta, the Shield forms the platform of crystalline basement rocks that floor the WCSB and is exposed in the East in Eastern Alberta, Saskatchewan and Manitoba (Ricketts, 1989). In Northeast Alberta, the Canadian Shield consists

of Archean and Proterozoic intrusive and metamorphic rocks that are strongly deformed (Buhlmann et. al., 2000). Also, the basement beneath the sediments of the WCSB is composed of deformed Archean and Proterozoic rocks. Geological, geochronological, geophysical and geochemical studies of exposed portions of the Precambrian Shield in North America have shown that the Shield is made of a tectonic collage of Archean crustal blocks separated by Proterozoic rocks that originated from orogeny and are interpreted as zones of collision (Hoffman, 1989). The Precambrian basement is quite important because its structure influences depositional patterns in the WCSB.

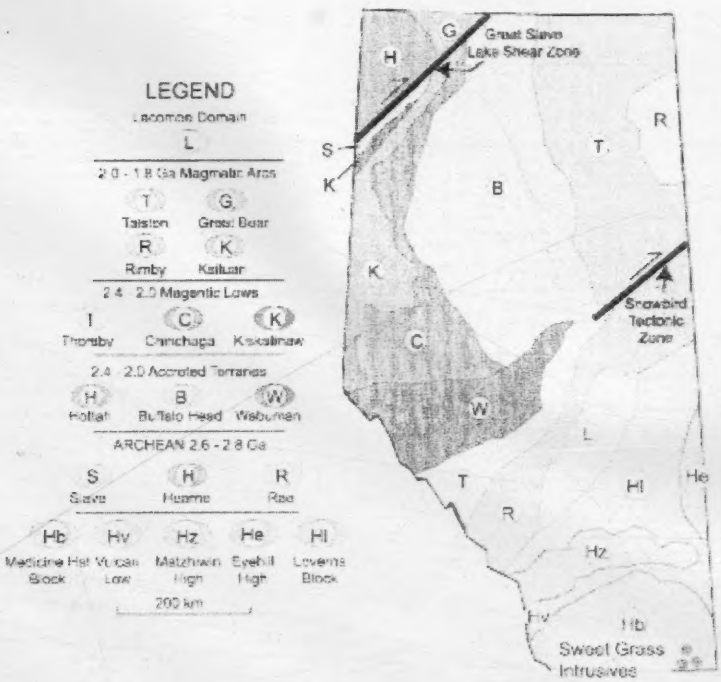

Figure 2.3: Map of exposed and subsurface basement terranes of Alberta. The study area is in the Medicine Hat Block region. (Modified from Ross et. al., 1991 and detailed documentation by Villeneuve et. al., 1993)

The major Precambrian basement domains of Alberta, such as the Archean Slave, Hearne and Rae Provinces are shown in Figure 2.3 (Ross et. al., 1991 and detailed documentation by Villeneuve et. al., 1993). These major domains can be further subdivided into unique crustal blocks, Proterozoic accreted terranes, magnetic lows, magmatic arcs and the Lacombe domain, which is of indeterminate origin. The Snowbird Tectonic Zone in central Alberta, the Great Slave Lake Shear Zone in northern Alberta, (both of which can be traced into the Shield) and the Vulcan Low, (a subsurface feature) are discontinuities, which subdivide the crystalline basement of Alberta. The study area is within the Medicine Hat Block.

2.2.2 Western Canadian Sedimentary Basin

The WCSB is one of the most prolific oil and gas-bearing basins in North America and consequently has become an area of enormous and continuous research and exploration. It is the largest basin in North America and covers parts of the United States of America (USA), Alberta (AB), Saskatchewan (SK), British Colombia (BC), Manitoba (MN), Yukon and the North West Territories (NWT). However, this section will focus on the WCSB within the Alberta Province (Figure 2.4).

The WCSB is an asymmetric basin, deepest in the west, floored with Proterozoic igneous and metamorphic rocks and. The basin is filled with a wedge of Phanerozoic sedimentary rocks that thickens from a zero edge in the east,

where the Canadian Shield is exposed, to the eastern edge of the Rocky Mountains (Figure 2.5). The sedimentary rocks attain a maximum thickness of approximately 6km in the southwest part of Alberta and range in age from Tertiary to the lowest Cambrian. These sedimentary deposits represent two main successions. The first is the Cambrian to mid-Jurassic underlying wedge (Porter et al., 1982) that consists of shale, platformal carbonates and evaporitic sediments with clastics sourced from the Canadian Shield to the east. The second is the Late Jurassic to Early Tertiary overlying Foreland Basin, dominated by clastic rocks sourced from the west.

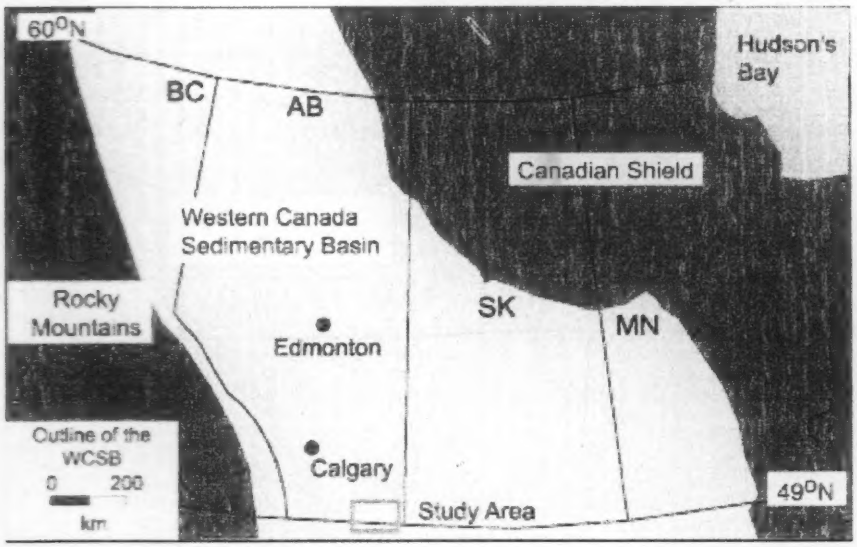

Figure 2.4: Location map showing the Canadian Shield, WCSB, Rocky Mountains and study area (not to scale) within Alberta, Canada

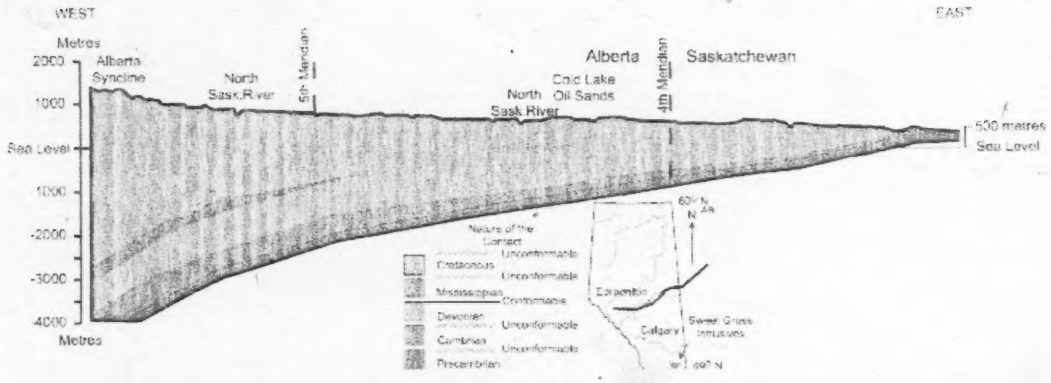

Figure 2.5: West to East crossection illustrating the thinning Phanerozoic wedge of the WCSB. (Modified from the Geological Atlas of the WCSB, Mossop & Shetsen, Chapter 3, 1994)

2.2.3 Phanerozoic Stratigraphy

Generally the study area has surface rocks mainly of the Quaternary age overlying cretaceous interbedded shales and sandstones. Carbonate rocks dominate the middle of the Phanerozoic profile and overlay largely siliclastic rocks of the Cambrian Period. Offsetting the seismic section (Chapter 4) is a well, BA H.B. Verdigris (Figure 2.7), the logs from which are used to generate a synthetic seismogram. A number of formations are behind the surface casing of this well and hence the tops approximately 200m are not logged (Figure 2.6). These will be briefly discussed (Meyboon. 1960). The formations are listed in chronological order from geologically latest to earliest. Figure 2.6 shows formations from the Quaternary Period to the Lower Cretaceous and Figure 2.7 continues from the Lower Cretaceous to the Cambrian.

<table>
<tr><th>Era</th><th>Period</th><th colspan="2">Formation</th></tr>
<tr><td rowspan="2">Cenozoic</td><td>Pleistocene</td><td colspan="2">river gravels, glacial deposits</td></tr>
<tr><td>Tertiary</td><td colspan="2">conglomerates, shales, sandstones</td></tr>
<tr><td rowspan="9">Mesozoic</td><td rowspan="7">Upper Cretaceous</td><td colspan="2">St. Mary River</td></tr>
<tr><td colspan="2">Bearpaw</td></tr>
<tr><td colspan="2">Oldman</td></tr>
<tr><td colspan="2">Foremost</td></tr>
<tr><td colspan="2">Pakowki</td></tr>
<tr><td colspan="2">Eagle / Milk River SS</td></tr>
<tr><td rowspan="4">Colorado</td><td>1st White Specks</td></tr>
<tr><td rowspan="2">2nd White Specks</td></tr>
<tr><td rowspan="2">Base Fish Scale</td></tr>
<tr><td rowspan="2">Lower Cretaceous</td><td rowspan="2">Bow Island SS</td></tr>
<tr><td>Basal Colorado</td></tr>
</table>

Figure 2.6: Stratigraphic column for southern Alberta up to the first formation below the surface casing. (Modified from Meyboom, 1960).

Pleistocene stage of the Quaternary Period

The majority of the Milk River area is covered by glacial drift of variable thickness, excluding the Cypress Hills area that was not scoured by glacial activity. However, in coulees this drift cover has been eroded thus exposing the Cretaceous strata that will be discussed later.

Tertiary Period

Tertiary deposits in this study area, with the exception of Cypress Hills, have been removed by erosion. In the Cypress Hills area sandstones and shales underlie conglomerates. No Tertiary deposits remain at the field site.

Cretaceous Period

St. Mary River Formation

The St. Mary River Formation consists of shales and thin sandstones and conformably overlays the Bearpaw Formation.

Bearpaw Formation

This formation is comprised mainly of shale interbedded with thin layers of bentonite and zones of iron nodules. It conformably overlays the Oldman Formation.

Oldman Formation

The Oldman Formation conformably overlays the Foremost Formation and is characterized by light-colored, sandy shales with some coal seams in the upper portion.

Foremost Formation

This formation contains gray and dark gray shales, coal seams, thin sandstone and some shell bearing beds. It conformably overlays the Pakowki Formation.

Pakowki Formation

The Pakowki Formation is composed mainly of gray shale with thin layers of ironstone, silty shale and bentonite. The top of this formation is quite difficult to differentiate from the lower beds of the Foremost Formation due their similarity. The Pakowki Formation conformably overlays the Eagle Formation.

Eagle Formation

This formation lays conformably upon the Milk River sandstone and is essentially a basal sandstone overlain by a series of interbedded shales, sandy shales and thin sandstones.

Milk River Sandstone Formation

This formation is indigenous to the study area and is exposed along the Milk River in Southern Alberta due to uplift of the Sweetgrass Arc. It consists of shales, minor siltstone and sandstone and is conformable with the underlying First White Specks.

First White Specks Formation (Figure 2.7)

The First White Specks of the Upper Cretaceous is the first formation exposed below the surface casing and contains dark gray shales, minor siltstone and sandstone. Both the First White Specks and the Second White Specks (discussed below) were named by Drillers who observed calcareous white specks in the shales. It is the upper boundary of the Colorado Group with the Milk River

Sandstone above it and the Medicine Hat Sandstone conformably below. On the gamma ray log it shows up as radioactive due to a high uranium content.

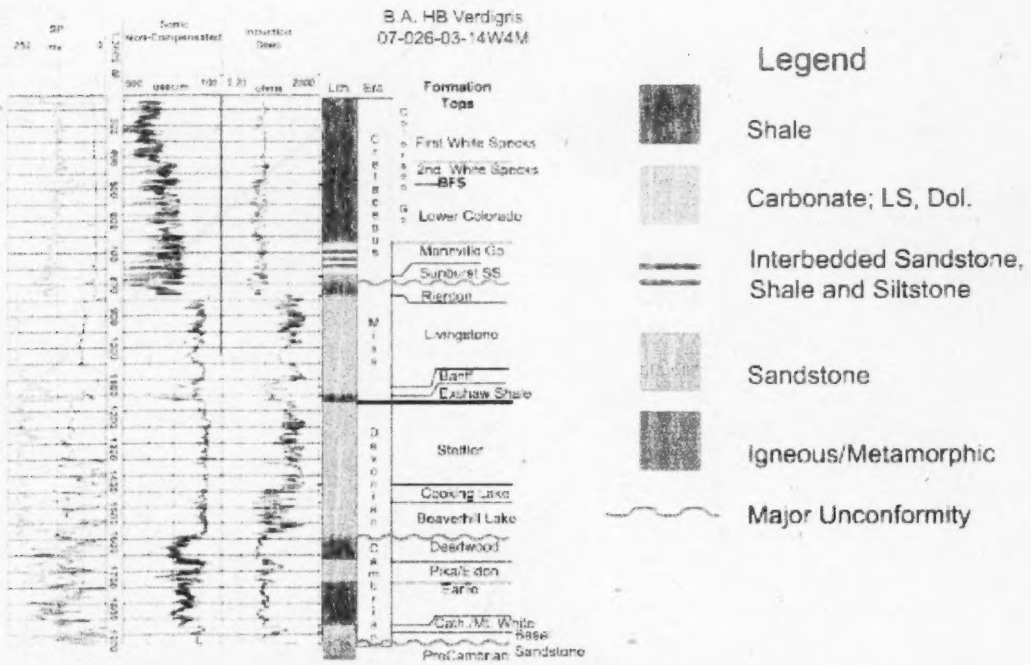

Figure 2.7: The Stratigraphic chart for the B,A. HB Verdigris well log approximately 1.2km NE of the study area. Formations from below the surface casing to the Cambrian Period

Second White Specks Formation

This formation is part of the Colorado Group and was deposited during the Late Upper Cretaceous Period. Like the First White Specks it contains shales, minor siltstone and sandstone. It is overlain by the First White Specks and is conformable with the underlying Base of the Fish Scales Formation. This Formation is characterized by high organic carbon content and radioactivity (again due to high uranium content) in well logs.

Base of the Fish Scales Formation

Base of the Fish Scales Formation is thought to have been deposited during the Early Lower Cretaceous Period (approximately Mid Cretaceous in age) and is also part of the Colorado Group. It is a marker bed that demarcates the Lower/Upper Cretaceous boundary, and is commonly used as a stratigraphic datum in geological projects. The Base of the Fish Scales Formation, like the First and Second White Specks, contains shales, minor siltstone and sandstone. However, it also contains abundant fish remains such as scales and skeletons, hence its name, and has a high organic carbon content. The Lower Colorado Shale conformably underlies this formation.

Lower Colorado Shale

The Lower Colorado shale is part of the Colorado Group and is dominantly composed of shales that lay unconformably on the Mannville Group.

Mannville Group

The Lower Cretaceous Mannville Group generally contains interbedded marine and non-marine shale, siltstone and fine-grained sandstone. A minor unconformity (i.e. very little rocks have been eroded) occurs at the top of the Mannville Group

Sunburst Member

The Sunburst member is dominantly composed of sandstone and is part of the Lower Cretaceous Mannville Group. It lays unconformably on the Rierdon Formation.

Mississippian (Carboniferous)

Reirdon Formation

The Rierdon Formation is within the Fernie Group; it contains shales and is partly calcareous with minor limestone interbeds. The Rierdon Formation conformably rests on the Livingstone Formation.

Livingstone Formation

The Lower Carboniferous (Mississippian) Livingstone Formation is within the Rundle Group and comprises carbonates, mainly clean limestone and dolostone. This formation conformably overlies the Banff Formation.

Banff Formation

The base of the Banff Formation contains a very thin layer of black shale overlain by a thicker layer of mixed carbonates and clastics which include marlstone, very argillaceous limestone and dolostone. Above this is a much thicker layer of cherty and silty argillaceous limestone and dolostone. The Banff Formation is of Lower Carboniferous age and conformably overlays the Exshaw Shale Formation.

Exshaw Shale Formation

The Lower Carboniferous is a black, organic-rich shale with minor silty to argillaceous sandstone, sandy siltstone, very sandy and silty dolostone. A minor unconformity may occur between the Exshaw Shale Formation and the Stettler Formation.

Devonian Period

Stettler Formation

The Upper Devonian Stettler Formation is comprised mostly of carbonates and anhydrites. This formation occurs conformably over the Upper Devonian Cooking Lake Formation.

Cooking Lake Formation

The Cooking Lake Formation, which conformably overlies the Beaverhill Lake Group is composed mostly of shelf carbonates and equivalent basin-filling shale. Limestones are the predominant carbonate.

Beaverhill Lake Group

The Beaverhill Lake Group lays unconformably on the Cambrian Deadwood Formation. It is the start of the Devonian Period containing open marine carbonates and covers most of the WCSB.

Cambrian Period

Deadwood Formation

This formation is Late Cambrian in age, and consists of interbedded shales and siltstones. It conformably overlies the Pika Formation.

Pika Formation

The Pika Formation comprises mostly limestones and dolomites. It is usually used as a marker bed to locate the overlying Deadwood formation and the underlying Earlie Formation. However, in our area the underlying Formation is the Eldon Formation. This Formation is of late Middle Cambrian in age.

Eldon Formation

This Formation is quite thin and consists mostly of carbonates - probably argillaceous limestone. Its age is Middle Cambrian and conformably overlies the Pika Formation. However, to the West (Rocky Mountains) it is a massive carbonate unit.

Earlie Formation

This Earlie Formation may actually be the Stephen Formation from the West. This Middle Cambrian Formation is composed of sequences of interbedded siltstone, fine-grained sandstone and shales, conformably overlying the Cathedral Formation.

Cathedral Formation

This carbonate-bearing formation conformably overlies the Mount Whyte Formation and is of Middle Cambrian age. Like the Eldon Formation it transforms into a massive carbonate unit in the West.

Mount Whyte Formation

The Mount Whyte Formation is of Middle Cambrian age composed of fine-grained clastics, mostly shales that are interbedded with limestone, minor sandstone and siltstone and is characterized by a relatively high gamma ray response. Interestingly, this formation is only mapped wherever the overlying Cathedral Formation exists. The Basal Sandstone Formation conformably underlies this formation.

Basal Sandstone Formation

These are Cambrian clastics lying unconformably on the Precambrian crystalline basement. The Basal Sandstone consists mainly of coarsed grained rocks and ranges in thickness up to 115m.

2.3 Igneous Intrusions

2.3.1 Sweetgrass Intrusives (SGI)

The most important tectonic feature neighbouring the study area is the 'Sweet Grass Intrusives' (SGI), which are northern outliers of the Sweetgrass Hills (SGH) situated in Southern Alberta and Northern Montana. Figure 2.8 shows the SGI (red star in dotted box) relative to the SGH (red circle in dotted box). The Sweetgrass Hills lay in the Medicine Hat Block region of the Montana alkaline igneous province, which is north of the Great Falls Tectonic Zone – GFTZ. The GFTZ separates the Archean Wyoming Block to the south and the Medicine Hat block to the north. The Sweetgrass Hills are considered to be a series of igneous intrusions on the east flank of the Sweetgrass Arch (see Section 2.3.2).

The SGI consists of dykes and plugs as well as an extrusive vent complex and are located approximately 12km southeast of the study area. Whole rock and trace element chemistry, mineralogy and mineral chemistry have shown that the rocks in these hypabyssal features are mainly minettes and that these minettes are similar to those found in the Montana alkaline province (Kjarsgaard, 1994). Minettes are defined as "mica traps" (Dawson, 1884), i.e., igneous rocks that consist of phenocrysts of olivine, phlogopite and diopside in a groundmass of mica, salite, sanidine, magnetite and apatite with lesser amounts of calcite and apatite (Kjarsgaard 1994). Geochemical data for the minettes in the Milk River

area provide evidence to suggest that they are similar to the rocks from the Archean Wyoming craton, which are mantle derived (Buhlmann et. al., 2000). Therefore by correlation the hypabyssal intrusive rocks in the study area can be classified as minettes that originated from the mantle (>100km).

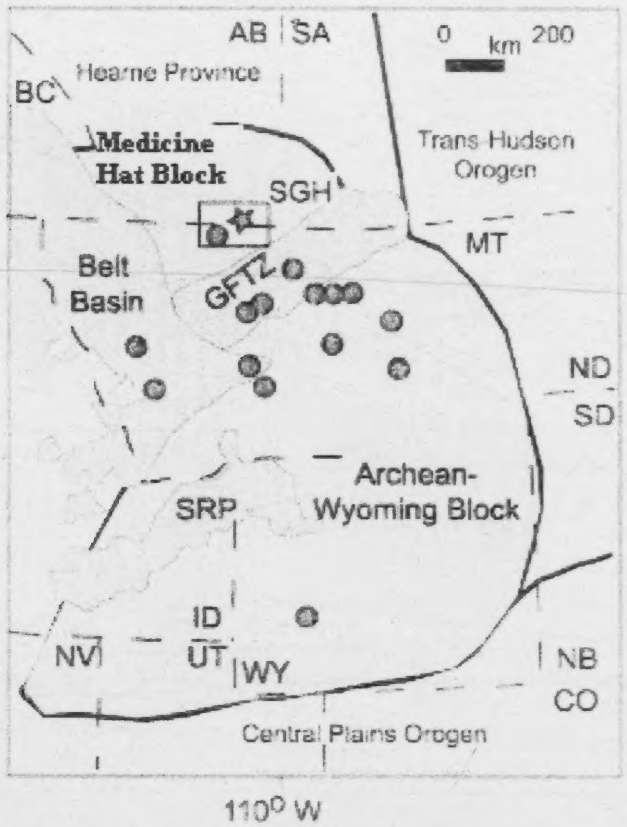

Figure 2.8: Location map for northwestern United States showing the SGI (red star in dotted box), Sweetgrass Hills (red circle in dotted box) in the Montana alkaline igneous province, the Archean Wyoming cratonic block and GFTZ. (Modified from Buhlmann et. al., 2000).

The SGI are essentially shallow mafic potassic-rich magmatic rocks of Eocene (49-53 Ma) age that range in composition from calcalkaline diorite

porphyry to mafic ultrapotassic rocks (Kjarsgaard, 1997 and Marvin et. al., 1980). The anomalies in the study area by extension could also be hypabyssal intrusives of the Eocene age.

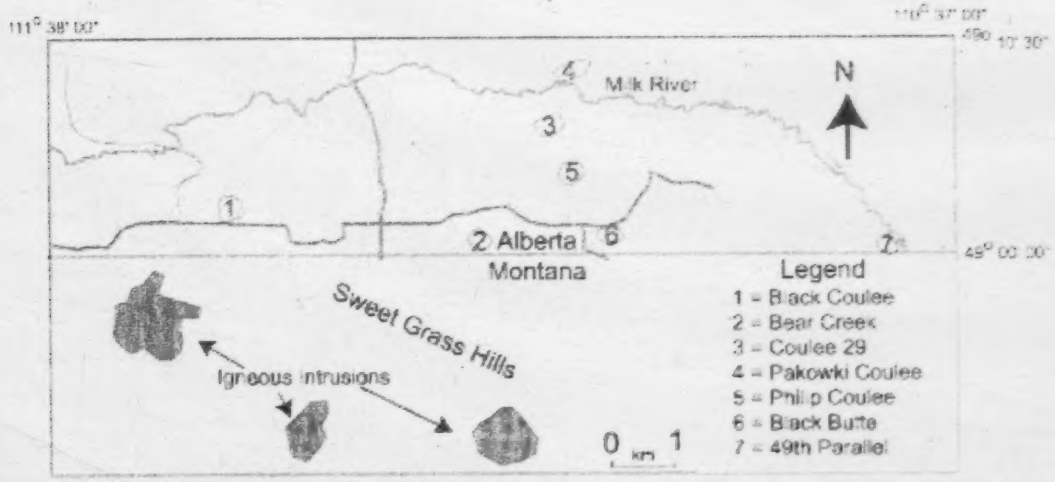

Figure 2.9: Location map showing the SGI in the Milk River area, southern Alberta, as well as, the Sweetgrass Hills in Montana. The SGI is approximately 12km southeast of the study area. (Modified from Kjarsgaard, 1994)

There are seven areas in Southern Alberta where Kjarsgaard, 1994, described the SGI outcrops. These outcrops are as follows (Figure 2.9):

1. Black Coulee
2. Bear Creek
3. Coulee 29
4. Pakowki Coulee
5. Philp Coulee
6. Black Butte
7. 49th Parallel

Black coulee

This outcrop is a grey hypabyssal (generic term for dykes, plugs and sills) mass that intrudes the sedimentary rocks of the Milk River Formation. Unlike the other six localities the rocks in this area are classified as diorite porphyry (andesite). The Black Coulee locality is found approximately 250m north of the Coutts-Aden road (highway 500). It outcrops below the eastern rim of the upper part of the Black Coulee.

Bear Creek

This is a minette dyke that intrudes the sedimentary rocks of the Foremost Formation. There are various portions of phlogopite, diopside phenocrysts and olivine within this dyke. This dyke is almost vertical with a due north strike and outcrops intermittently over 1.1km in shallow Coulees east of Bear Creek. The two best exposures average 75m in length and 2m in width.

Coulee 29

An irregularly shaped minette vent complex exists in this locality and is characterized by at least four major magmatic events, which intruded in the sedimentary rocks of the Pakowki and Foremost Formations. This Coulee occurs at the southern edge of the Milk River Valley rim (Burwash 1992). The minette pyroclastics in this area are the only known locality where extrusive rocks are preserved in the Sweet grass Hills.

Pakowi Coulee

The Pakowki Coulee minette dyke/plug is an irregular mass, averaging 25m x 20m in size that intrudes the sedimentary rocks of the Pakowki Formation. This dyke/plug rises to approximately 10m above the level of Milk River and is north of the river. The characteristic brown minette rocks in this are similar to those in Coulee 29.

Philp Coulee

This minette dyke has a strike of approximately 029° with sub vertical dips and intrudes the Oldman Formation in an en-echelon (overlapping or staggered arrangement) fashion and averages 1 to 3m in width. The southern portion to the middle of the 700m long dyke is well exposed at three locations in 40-100m sections whereas in the northern portion of the dyke there is little exposure.

Black Butte

A large minette plug is at this locality, which rises approximately 30m above the surrounding plains, intruding the Oldman Formation. This plug exists in plan view as a stretched ovoid with a long axis trending northeast/southwest and having dimensions of about 400m x 200m. Dark to light grey minette intrusives are usually exposed.

49th Parallel

The 49th Parallel locality includes four minette dykes that intrude the Foremost and Oldman Formations. This locality is the most easterly of the seven and is between Milk River and the Canada-USA border. There is one major dyke and three minor ones north and sub parallel to it. The main dyke has a sub vertical dip, a strike of 055° and width ranging 1 to 2m whereas the three other dykes are thinner, with widths ranging from 0.5 to 1m, and strikes ranging 051° to 073°. The main dyke is exposed for approximately 90m continuously and then intermittently over about the next 110m.

In short there appears to be a number of dyke-like igneous features in the vicinity of the SGH and these features are most likely related to the SGH. The outcrops are quite limited but hint that a great deal of the remaining intrusives are buried. A major purpose of this of this study is to attempt to better understand some of these buried features.

2.3.2 Sweetgrass Arc

The Alberta plains region is located on a northeasterly structurally trending positive element known as the Sweetgrass Arc extending from central Montana into southeastern Alberta. The Sweetgrass Arc includes the Bow Island Arc and separates two major Basins, the Williston and the Alberta Basins, described in Section 2.2.1 (Figure 2.2). The Sweetgrass Arch is thought to exist as a result of

primary tectogenesis (differential vertical movements of the basal complex) and not compressional forces and this is reflected in the overlying mantle of sediments (Meyboon 1960). Consequently, this process produced the Kevin Sunburst Dome and the Bow Island Arc. Plutonic activity associated with this primary tectogenesis produced the Sweetgrass Hills intrusions.

The study area occurs in the proximity of the SGI; the SGI are located in the Kevin-Sunburst Dome at the southwestern edge of the Bow Island Arc (Figure 2.2). The Kevin-Sunburst Dome is northwest trending unlike the northeast trending Bow Island Arc.

2.4 Summary

The geological overview of Alberta and the study area was necessary in order to model and interpret the magnetic and seismic data collected by the Field School class of the University of Alberta in the Milk River area.

Knowledge of the WCSB and the Precambrian Shield, which the WCSB rests upon, was a prerequisite in studying an area within Alberta. The Phanerozoic stratigraphy using the well, B.A.HB Verdigris located 1.2km northeast of the study area, past geological data (Meyboon, 1960) and the Geological Atlas of the Western Canadian Sedimentary Basin (Mossop & Shetsen, 1994) was vital in modelling and interpreting the seismic reflection data collected.

Geochemical studies performed by Kjarsgaard, 1994 on rock samples from the SGI, which represent the northernmost extension of the Sweetgrass Hills showed that these rocks are minettes and are similar to those in the Sweetgrass Hills of the Montana alkaline province. Geochemical studies on the minettes in Milk River area provided evidence that these minettes were similar to the mantle derived minettes in the Archean Wyoming Craton (Buhlmann et. al., 2000). Therefore the intrusive rocks in the study area may be minettes that originated from the mantle. Also, the SGI are of Eocene age and the hypabyssal features of the neighbouring study area may be considered to be of the same age.

Additionally, the anomalies in the study area are postulated to be analogous to the dykes and sills that outcrop in the SGI. Kjarsgaard, 1994, described these outcrops Black Coulee, Bear Creek, Coulee 29, Pakowki Coulee, Philp Coulee, Black Butte and 49th Parallel in some detail.

Chapter 3

Magnetic Data

3.1 Introduction

In geophysical surveys an airborne or a ground magnetic survey is typically performed as a preliminary to seismic profiling in order to determine the approximate depth, topography and character of subsurface rocks. In this instance, a high resolution ground magnetic survey was carried out using the University of Alberta's GSM-19 Overhauser Proton Precession Magnetometer shown in Figure 3.1. This ground magnetic survey was motivated by past geophysical (aeromagnetic survey carried out in the 1990's by the Geological Survey of Canada and past ground magnetic surveys performed by the University of Alberta's Field School) and geological studies (as described in chapter 2 of this

thesis) in southern Alberta. These studies revealed the presence of many dykes in the southern Alberta area (Kjarsgaard, 1994) and the imaging of these dykes are the focus of the magnetic surveys.

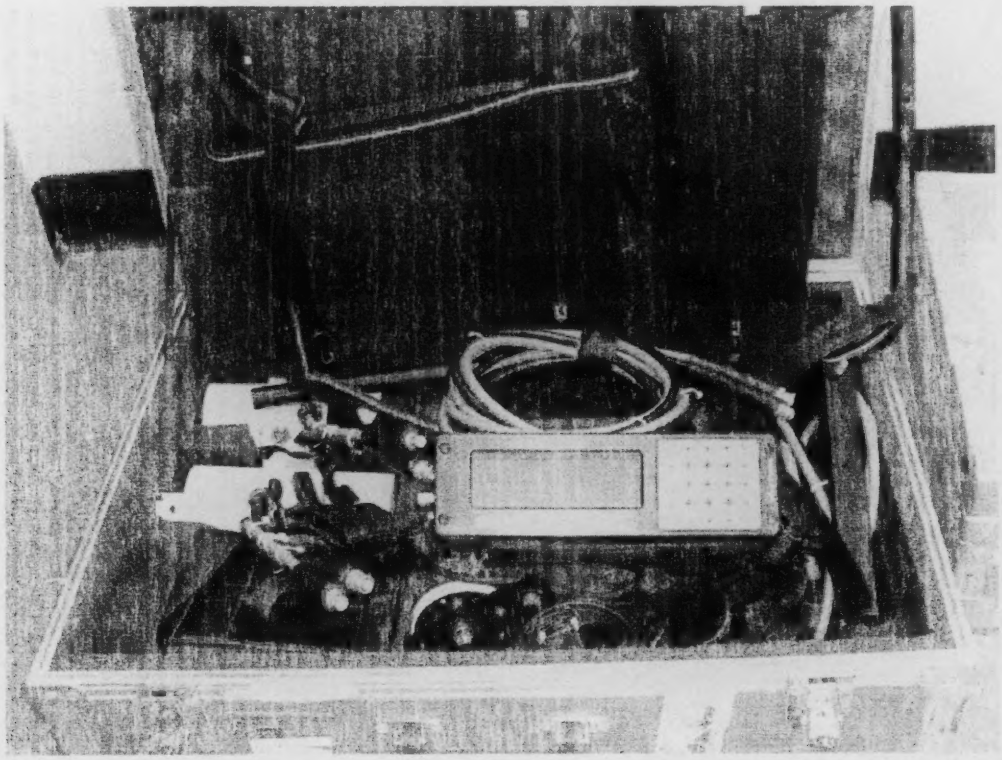

Figure 3.1: The University of Alberta GSM-19 Overhauser Proton Precession Magnetometer.

The ground magnetic survey was carried out in August 2001 over an area of approximately 1.6km by 1.3km in the north-south and west-east directions respectively (Figure 1.2 in Chapter 1). The magnetic data set obtained was subsequently processed using the processing flow described in Figure 3.5, imaged

in Matlab and modeled using "Potent", a modelling software designed by Geophysical Software Solution (http://www.geoss.com.au/).

3.2 Background

The inclusion of the magnetics in this thesis was inspired by research work done by Ross et. al., 1996 in the region referred to as Cypress Hills survey area (Figure 3.2) in southern Alberta. This work was based on the high-resolution aeromagnetic data collected by the Geological Survey of Canada (GSC) in the fall of 1992 over the Cypress Hills survey area.

The Cypress Hills survey confirmed the long wavelength basement sourced anomalies interpreted from an earlier survey in the 1960s done by the GSC (Ross et. al., 1996) and funded by PanCanadian Petroleum Limited. In addition, the aeromagnetic data from the Cypress Hill survey revealed the existence of unusually shallow, high wavenumber anomalies which Ross et. al, 1996, modeled and speculated as to origin of these anomalies. The northwest trending long wavelength anomalies were prevalent in the aeromagnetic anomaly map for the Cypress Hills survey area (Figure 3.3). Also, several relatively narrow northwest high wave number anomalies were observed between the town of Milk River and the city of Lethbridge (Figure 3.3). Ross et. al. 1996 proceeded to calculate the first vertical derivative of the total magnetic field in order to enhance

these shallow high wavenumber features (Figure 3.4). However, sometimes the derivative process tends to intensify the noise and so precautions should be taken with the interpretation of these anomalies. Figure 3.4 illustrates these high wavenumber anomalies, where the most dramatic anomaly appears as a series of relatively thin high wavenumber northwest trending features between Lethbridge and Milk River and another less obvious north trending anomaly was located south of Medicine Hat.

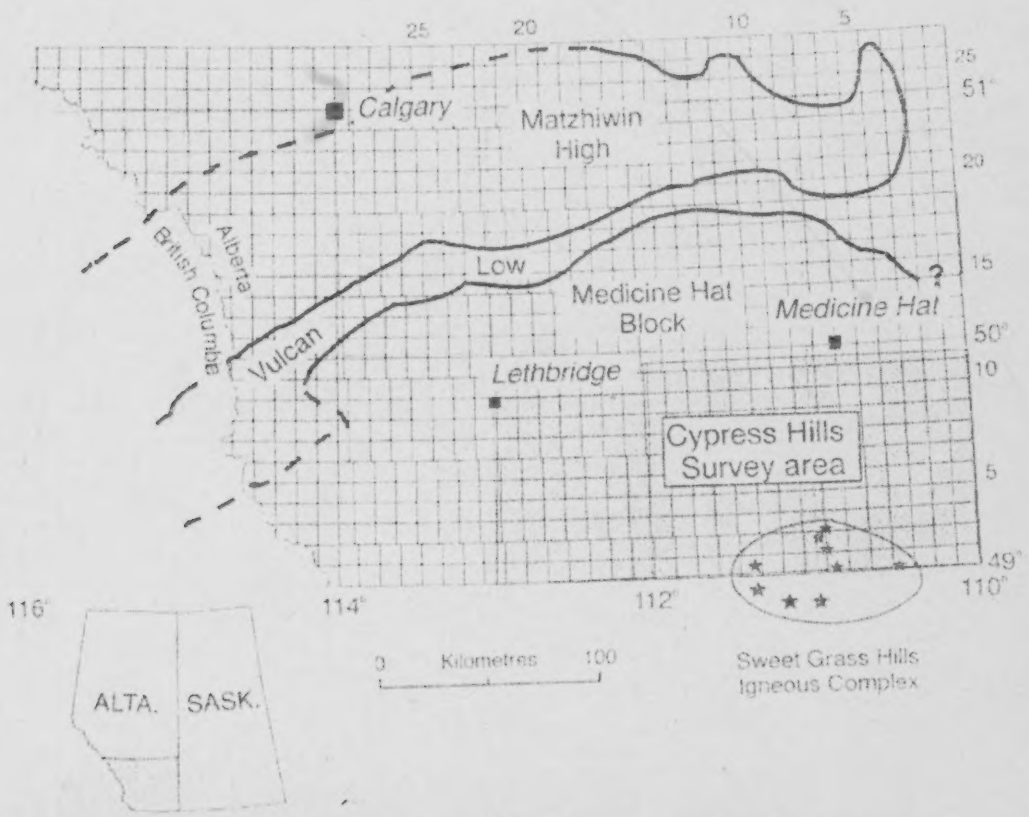

Figure 3.2: A location map showing the Cypress Hills survey area in southern Alberta where the GSC collected aeromagnetic data in the fall of 1992. The stars in the Alberta region are termed the Sweetgrass Intrusives (Kjarsgaard, 1994). Figure modified from Ross et. al., 1996

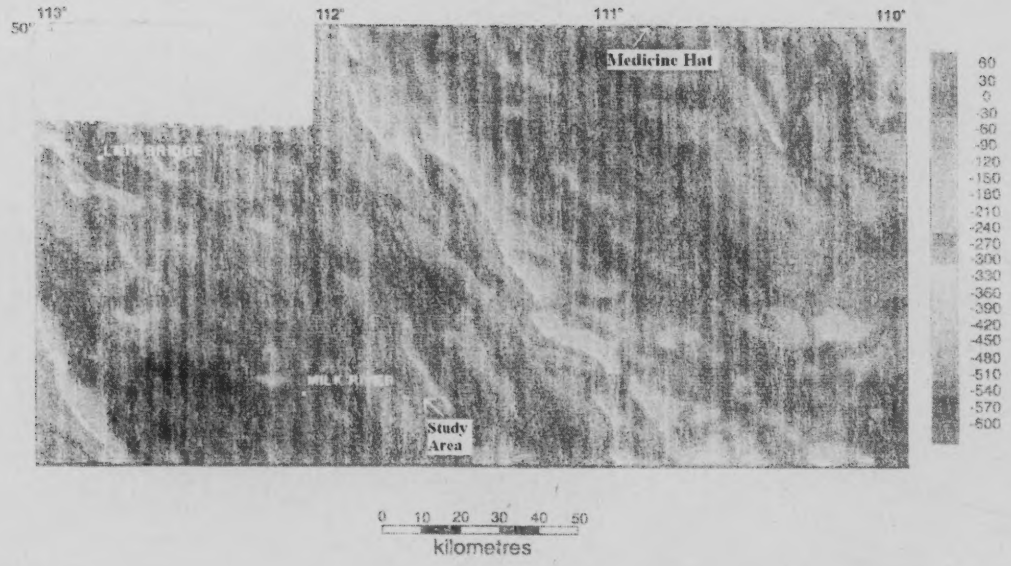

Figure 3.3: Total Intensity map for the Cypress Hills survey area. The International Geomagnetic Reference Field was removed for an altitude of 1.1km. Figure modified from Ross et. al., 1996

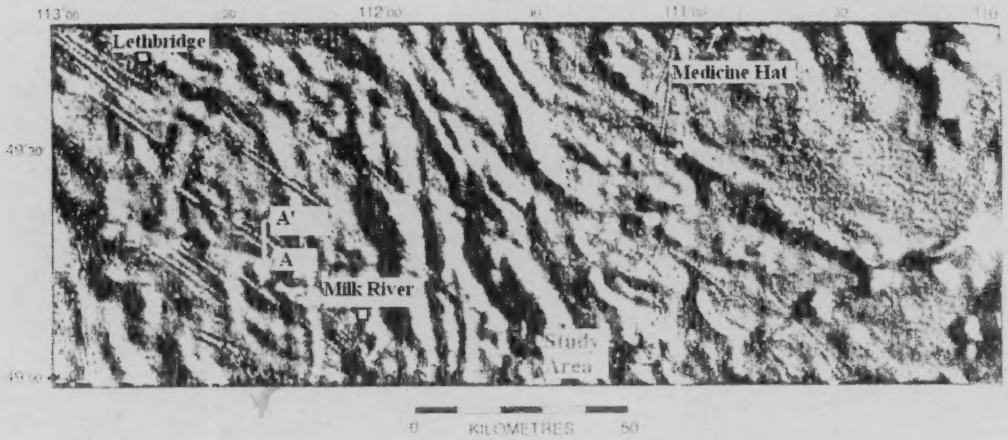

Figure 3.4: First vertical derivative of the total intensity aeromagnetic data. Figure modified from Ross et. al., 1996.

A ground magnetic survey was carried out along the profile AA' shown in Figure 3.4 (Ross et. al., 1996) south of Lethbridge. This ground magnetic survey was over a known high wavenumber anomaly. The data collected was upward continued to the elevation of the aeromagnetic survey and compared to the corresponding flight line. The ground and aeromagnetic surveys showed similarities with respect to wavelength, asymmetry and intensity, thus eliminating speculation that these shallow anomalies were due to acquisition artifacts or cultural sources.

Ross et. al., 1996 initially interpreted these linear shallow anomalies to represent shallow igneous dykes rather than magnetization along fault zones. This could be expected due to the presence of igneous rocks in southern Alberta and to the proximity of the Sweet Grass Intrusives described by Kjarsgaard, 1994 (as described in chapter 1 of this thesis). The Sweet Grass Intrusives consist of seven igneous outcrop localities in southern Alberta, south of Milk River and is part of the Sweet Grass Hills Igneous Complex. Six of the outcrops are intrusives that contain sills and dykes and the seventh is an extrusive vent. By correlation with the Sweet Grass Intrusives it can be speculated that these shallow anomalies represent dykes.

Ross et. al., 1996 went on to construct 2.5-D models, which indicated that the anomaly could be a dyke within the shallow sedimentary layers. Based on the modelling, magnetic response, linearity, swarm-like subparallel geometry and comparison with the mafic dykes in the Canadian Shield (Schwarz et. al., 1987 and West and Ernst, 1991), they concluded that these shallow anomalies are

indeed igneous dykes. These shallow anomalies are interpreted as being analogous with the Sweet Grass Hills complex and would therefore be of the Eocene age.

3.3 Acquisition

The magnetic data was collected by the Field School class of 2001 using the University of Alberta's GSM-19 Overhauser Magnetometer, a portable Proton-Precession Magnetometer. This Magnetometer records the total magnetic field strength in nanoTeslas (nT), that is, only information about the peak magnitude of the magnetic field- not direction - was obtained. The magnetometer operates based on the measurement of free-precession frequency of protons, which have been polarized approximately perpendicular to the direction of the Earth's magnetic field. Sudden removal of the polarizing field results in the precession of the protons about the Earth's magnetic field at the Larmor frequency (the frequency which is proportional to the magnetic field strength) and this is recorded (Telford et. al. et. al., 1990).

Magnetic readings were recorded along fifteen (15) north-south lines each of approximate length 1.6km. Successive lines were approximately 90m (100 paces) apart and an average of one reading per second was recorded continuously

along each profile line. A base station magnetometer was time- synchronized with the "recording magnetometer" to facilitate diurnal corrections.

The GPS x (East-West direction), y (North-South direction) and z (elevation) positions according to the Universal Transverse Mercator (UTM) Grid System were obtained using the University of Alberta's Trimble 4600 LS Differential GPS unit. The positions were recorded every 90m (approximation to 100 paces) along each line and subsequently they were integrated into the magnetic data set.

3.4 Processing

3.4.1 Methodology

The Matlab codes for processing the magnetic data were provided by Dr. M. Heimpel. These Matlab codes were modified to obtain outputs that were only necessary for this thesis. Figure 3.5 shows the processing flow that was used to process the magnetic data set.

Magnetic data reduction is usually an insignificant task with the exception of diurnal corrections. The effect of elevation is quite insignificant since the vertical gradient varies approximately 0.03nT/m at the poles to 0.01nT/m at the equator (Telford et. al. et. al., 1990). Latitude corrections were not carried out

since the latitude variation is rarely greater than 6nT/km (Telford et. al. et. al.. 1990) and the terrain corrections were not applied due the relatively flat nature of the survey area. However, diurnal corrections were applied by taking the magnetic base station readings simultaneously with the collection of magnetic data in the survey area, then subtracting the base station magnetic readings from the corresponding magnetic readings.

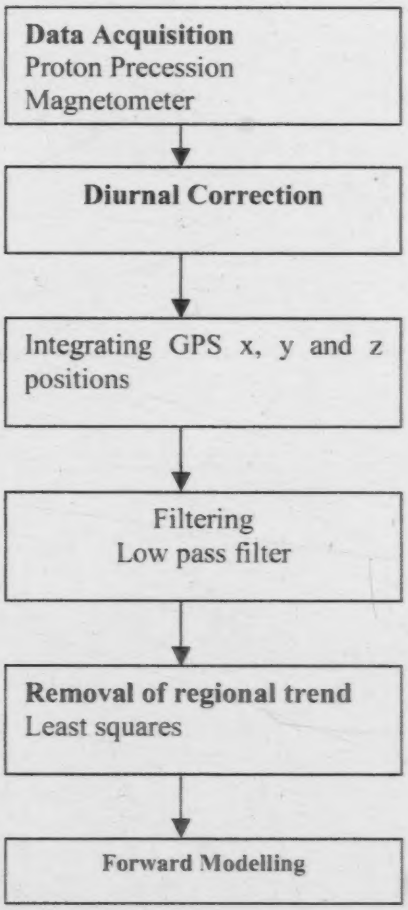

Figure 3.5: Processing flow for the magnetic data set.

The GPS positions were recorded at approximately 90m (100 paces) intervals and magnetic readings were taken every second (approximately every 0.7m). Therefore, a GPS reading was not taken for every magnetic reading and consequently the GPS x, y and z positions along each north-south line were interpolated.

A low pass filter was used to remove noise from the magnetic data (the high wavenumbers, i.e., $k_{mag}>7x10^{-4}$/m were removed from each magnetic profile line). This was especially necessary for the data recorded along the road where the reflection seismic survey was carried out (Figure 3.6(a)). The regional magnetic field was calculated using least squares and then removed from the entire magnetic data set. The magnetic profile lines were then interpolated onto a uniform grid and imaged (Figure 3.7). Finally, forward modelling using "Potent", a modelling software designed by Geophysical Software Solution (http://www.geoss.com.au/). was performed to interpret underlying geological structures. The 4th magnetic line east of the seismic line (that is, 510m east of the seismic line or 442943 east shown in Figure 3.6(e)) was used for comparison against the model magnetic data.

3.4.2 Results

All fifteen (15) profile lines were plotted against the northings (Figure 3.6(a) to 3.6(o)). The blue curve represents the diurnally corrected magnetic data and the red, the low pass filtered data. The difference in general shape of the magnetic

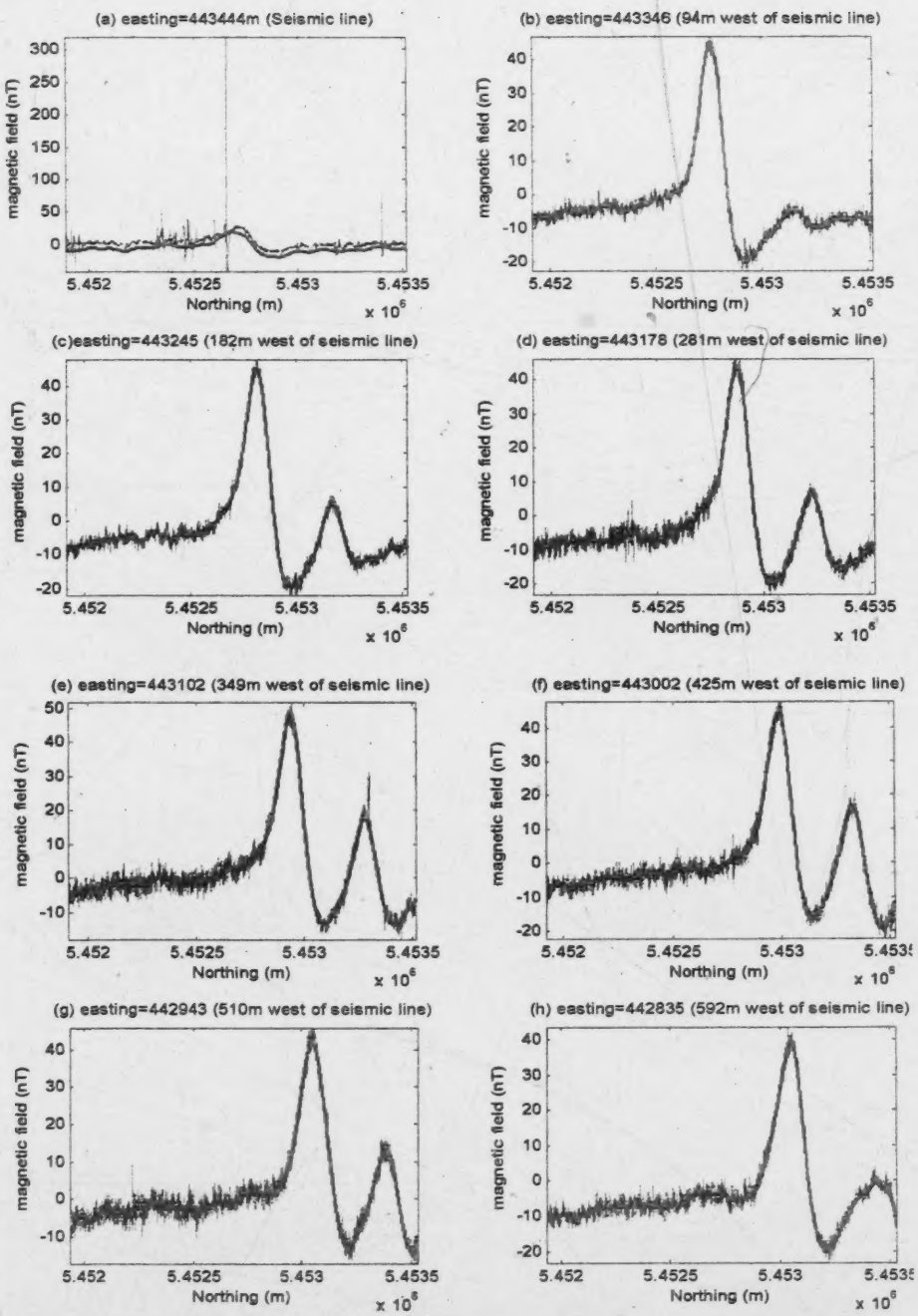
(a) easting=443444m (Seismic line)
(b) easting=443346 (94m west of seismic line)
(c)easting=443245 (182m west of seismic line)
(d) easting=443178 (281m west of seismic line)
(e) easting=443102 (349m west of seismic line)
(f) easting=443002 (425m west of seismic line)
(g) easting=442943 (510m west of seismic line)
(h) easting=442835 (592m west of seismic line)
magnetic field (nT)
Northing (m)
x 10^6
5.452
5.4525
5.453
5.4535

Figure 3.6 (a) to (h): Plot of the magnetic field (nT) versus profile lines south to North (left to right). The blue curve represents the diurnally corrected data and the red the low pass filtered data. (a) has vertical scale 1cm=100nT, (b) to (h) is 1cm=20nT. Horizontal scale is 1cm=300m.

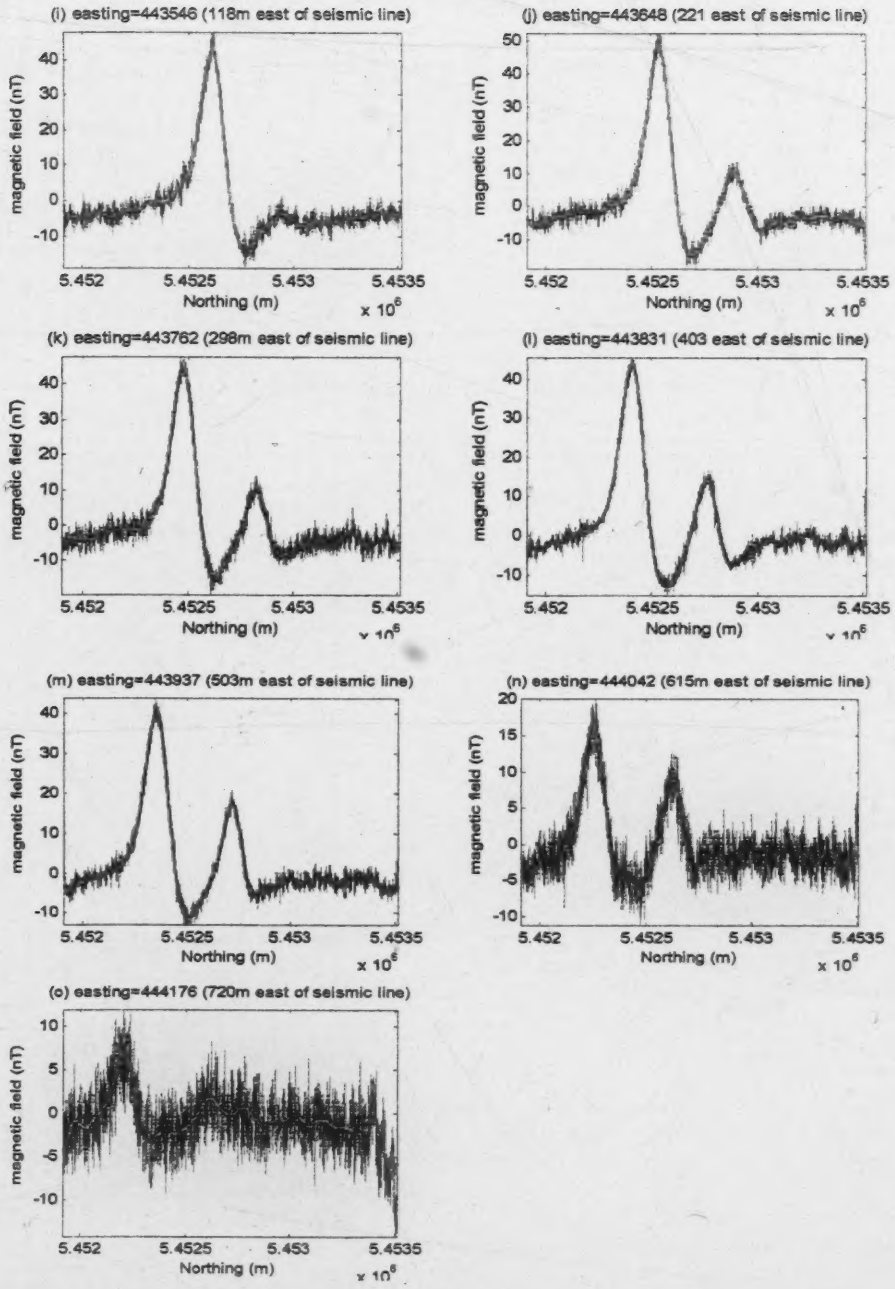
(i) easting=443546 (118m east of seismic line)
(j) easting=443648 (221 east of seismic line)
(k) easting=443762 (298m east of seismic line)
(l) easting=443831 (403 east of seismic line)
(m) easting=443937 (503m east of seismic line)
(n) easting=444042 (615m east of seismic line)
(o) easting=444176 (720m east of seismic line)
magnetic field (nT)
Northing (m)
x 10^6
5.452
5.4525
5.453
5.4535

Figure 3.6 (i) to (o): Plot of the magnetic field (nT) versus profile lines south to North (left to right). The blue curve represents the diurnally corrected data and the red the low pass filtered data. (i) to (m) is 1cm=20nT and (n) to (o) is 1cm=8nT. Horizontal scale is 1cm=300m.

Profile position	Reference Figure	Magnitude of southerly, anomaly (nT)	Magnitude of northerly anomaly (nT)
Seismic line (east 443444m)	3.6(a)	20	N/A
94m west of seismic line	3.6(b)	45	-4
182m west of seismic line	3.6(c)	45	5
281m west of seismic line	3.6(d)	45	6
349m west of seismic line	3.6(e)	48	17
425m west of seismic line	3.6(f)	45	16
510m west of seismic line	3.6(g)	42	13
592m west of seismic line	3.6(h)	40	-0.5
118m east of seismic line	3.6(i)	42	-3
221m east of seismic line	3.6(j)	48	10
298m east of seismic line	3.6(k)	46	10
403m east of seismic line	3.6(l)	44	14
503m east of seismic line	3.6(m)	40	17
615m east of seismic line	3.6(n)	16	9
720m east of seismic line	3.6(o)	7	2

Table 3.1: Position of the magnetic profile line relative to the central seismic line and the magnitudes of their anomalies.

profile along the seismic line (Figure 3.6(a)) and the others (Figures 3.6(b) to 3.6(o)) are quite evident. The magnetic profile along the seismic line on the road shows the presence of only one anomaly and was much more noisy whereas the other fourteen show two anomalies and is less noisy. In addition, the intensity of the lone anomaly along the seismic line is small, with a maximum amplitude of 20nT compared to an average amplitude 45nT for the corresponding anomaly (that is the more southernmost anomaly) of the other profiles, with the exception of the two most easterly profiles (Figures 3.6(n) to 3.6(o)) where the corresponding anomalies have smaller intensities of 16nT and 9nT, going from west to east. The second northernmost anomaly is of a much smaller intensity compared to the southernmost one and Table 3.1 illustrates the magnitude of these two characteristic anomalies along each profile line.

The final image of the magnetic data (Figure 3.7) collected after processing shows two linear subparallel northwest trending anomalies of average intensity of 45nT and 15nT and they appear to be discontinuous at the seismic line along the road. These anomalies are not overly large but are distinct nonetheless.

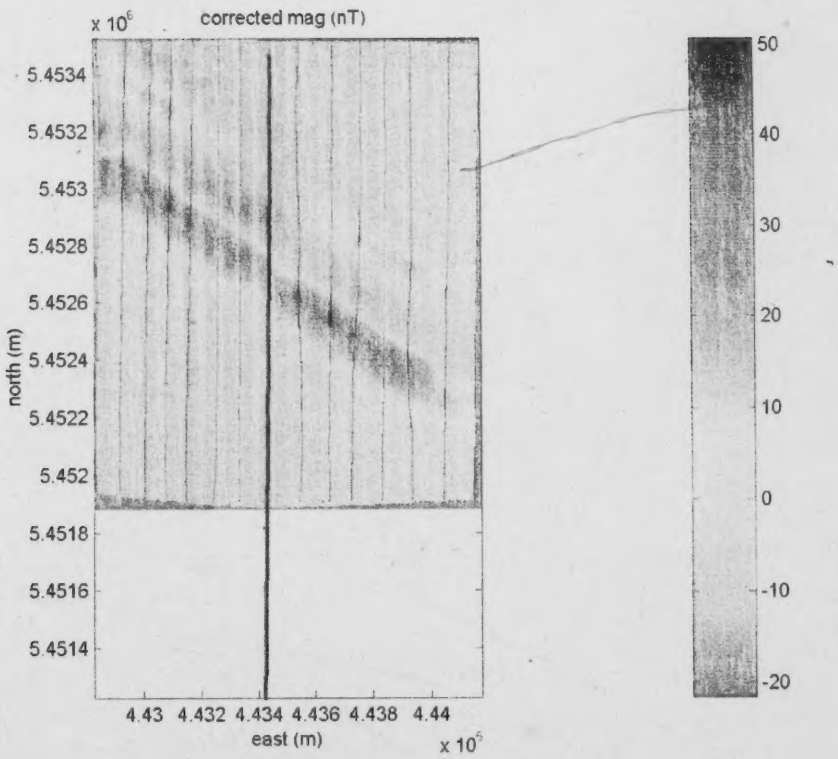

Figure 3.7: Image of processed magnetic data together with the seismic reflection survey coverage (central bold line, i.e., 8th profile line to the left). Vertical and horizontal scales is 1cm=200m

3.5 Modelling

"Potent", modelling software designed by Geophysical Software Solution for modelling magnetic data, was used in this section. Forward modelling was applied by manually adjusting model parameters in order to improve the fit between the observed data and the calculated data due to the model. Parameters such as strike

(direction of the dyke as it intersects the horizontal surface), dip (angle the dyke makes with the horizontal, measured perpendicular to the strike and in the vertical plane), magnetic susceptibility, width, length and depth from the surface were adjusted. An inducing field was obtained from a magnetic anomaly map with a main field strength of 57451nT, an azimuth of 15.2° and an inclination of 73° and was input into the software before carrying out the forward modelling.

The dyke models were chosen due the proximity of the Sweet Grass Intrusives, (Kjarsgaard, 1994) within the Sweet Grass Hills complex, which is 12km southeast from our study area and contains many dykes. The magnetic calculations for the 2D dyke/prism models were based on the common formulas for the anomalies due to a semi-infinite slab (Grant and West, 1965).

The observed magnetic data from the 4th profile line east of the seismic line (510m east of the seismic line) at UTM coordinate 442943 east was used to model the magnetic data (Figure 3.6(e)). Different 2D models are shown in Figure 3.8 to 3.10 and in each case the blue curve represents the observed data and the red curve the modeled data. The top graph in each figure represents a plot of total magnetic field intensity (TMI) in nT versus offset (P) in metres (originating from south and extending to the north) while the bottom graph represents depth (z) in metres versus northings (Y) in metres.

The first model (Figure 3.8) represents two (2) subparallel subvertical dykes with a strike of approximately N124°E and dip of approximately 63°SW. The larger of the two dykes (that is, the red, southerly dyke) is approximately 10m wide whereas the other dyke (that is, the black, northerly dyke) has a width of

approximately 5m. They are both at approximately 70m below the surface, i.e. z=-70m, and extend to depths beyond 2000m. The magnetic susceptibility (k) was another parameter that was varied such that the southerly dyke had a value of 0.025 and the other a value of 0.02. Magnetic susceptibility values were chosen based on measurements taken using a hand held Scintrex meter of rock samples from the SGI area by Kjarsgaard, 1994 and Ross et. al., 1996.

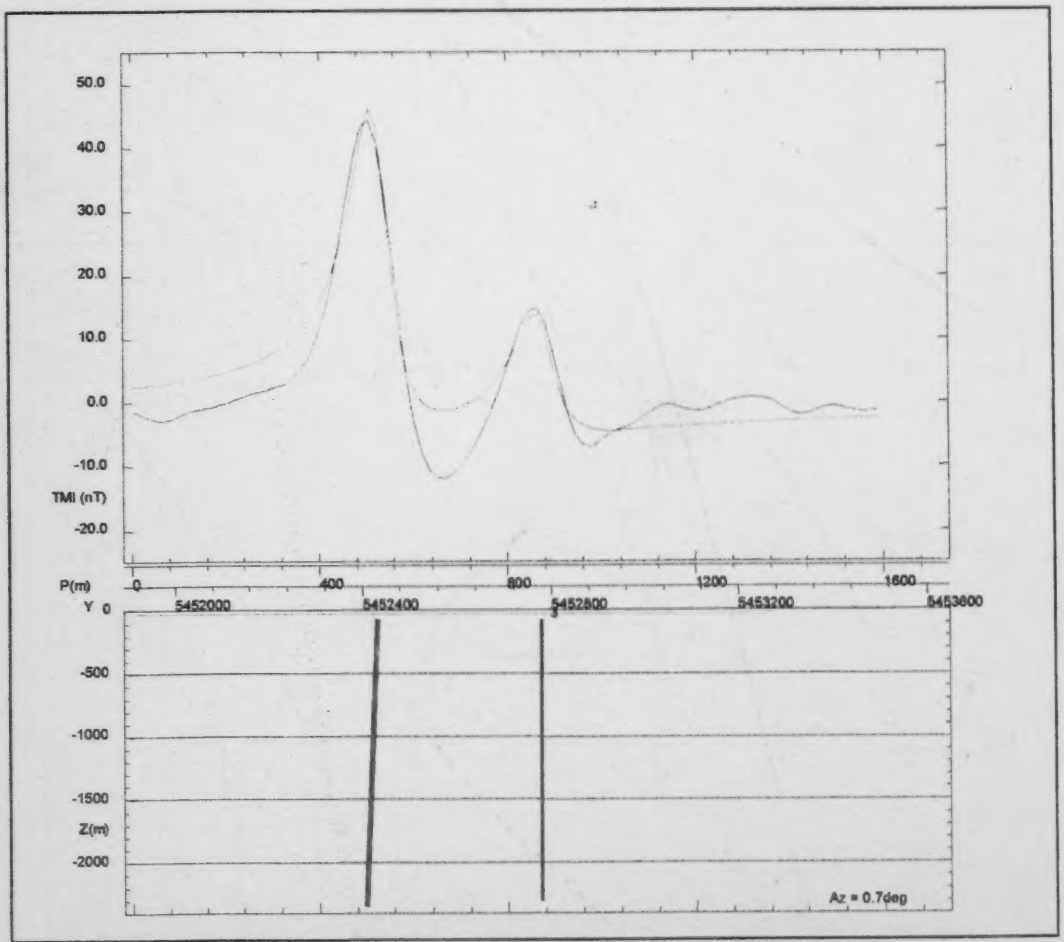

Figure 3.8: The blue line represents the observed data and the red the modeled data. Top graph is total magnetic field intensity, TMI (nT) vs. offset, P(m) and bottom graph is depth, z (m) vs. northings, Y(m). Larger southerly dyke (red): width=10m, k=0.025. The other dyke (black): width=5m, k=0.02. In both cases Z=-70m, strike and dip are N124°E and 63°SW respectively.

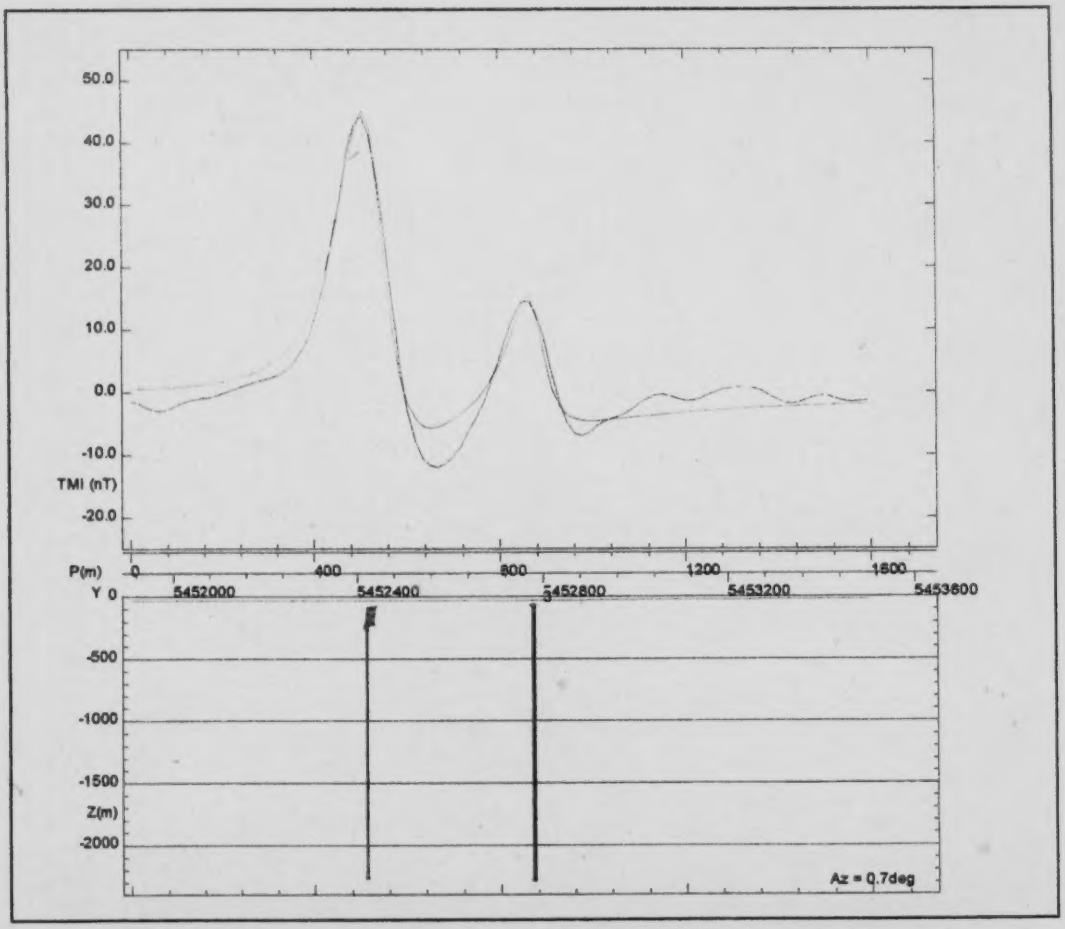

Figure 3.9: The blue line represents the observed data and the red the modeled data. Top graph is total magnetic field intensity, TMI (nT) vs. offset, P(m) and bottom graph is depth, z (m) vs. northings, Y(m). The southerly dyke, Z=-80m, width and k of red portion is 4m and 0.025 and width and k of the green portion is 20m and 0.02 respectively. The other dyke (black): z=-65m, width=5m and k=0.02. In both cases, strike and dip are N124°E and 63°SW respectively.

In the second case (Figure 3.9) the model appears to be a better fit to the observed data. However, in this instance the southerly dyke thickens to the top (green portion) and the other dyke is regular in width (black). Similarly with the previous model they are both subparallel and subvertical with the strike and dip approximately N124°E and 63°SW respectively. The most southerly dyke

thickened from a width of 4m at a depth greater than 2000m to 20m at an 85m depth whereas the other dyke had a width of 5m and extended from 65m to beyond 2000m depths. The magnetic susceptibility (k) for the thickening dyke was 0.025 at the bottom to 0.02 at the top and 0.02 for other dyke.

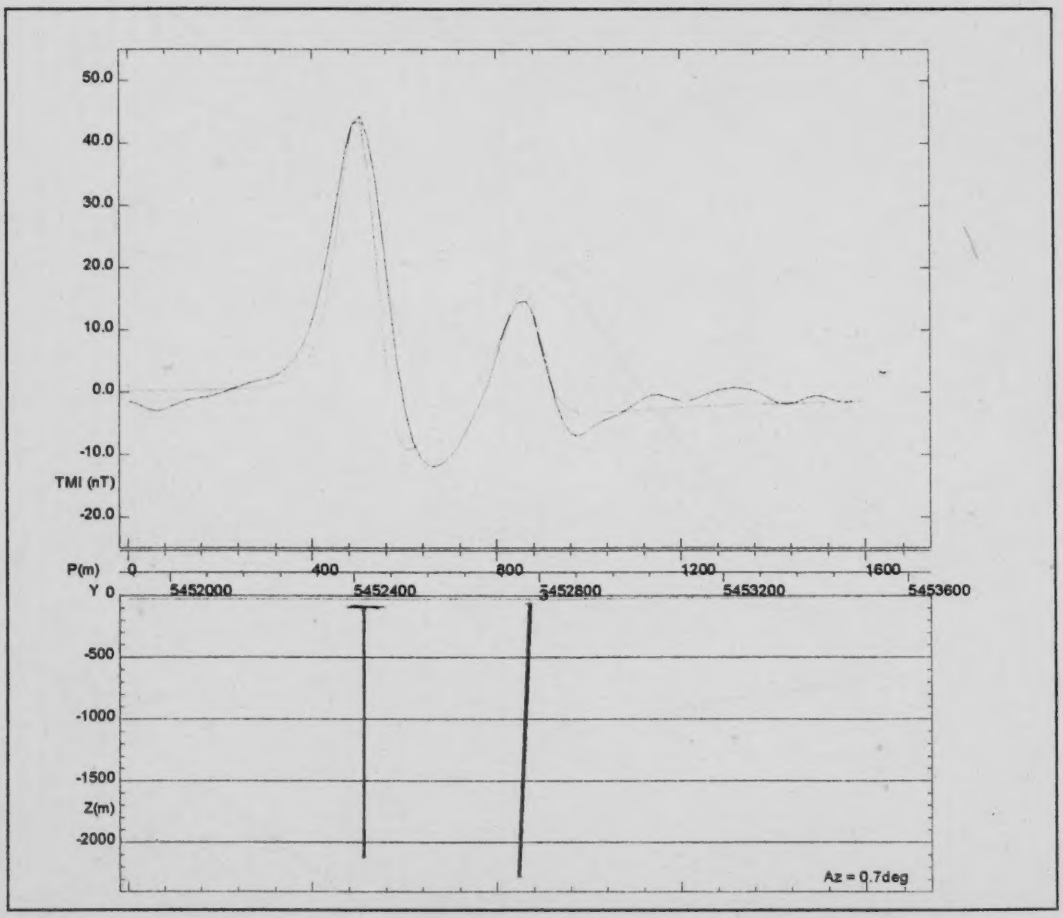

Figure 3.10: The blue line represents the observed data and the red the modeled data. Top graph is total magnetic field intensity, TMI (nT) vs. offset, P(m) and bottom graph is depth, z (m) vs. northings, Y(m). The southerly dyke, Z=-85m, width and k of red portion is 4m and 0.015 and width and k of the green portion is 20m and 0.02 respectively. The other dyke (black): z=-65m, width=5m and k=0.02. In both cases, strike and dip are N124°E and 63°SW respectively.

The third model does not fit the data as well as the previous, however it could possibly exist. The southerly dyke which extends from a depth of 85m to beyond 2000m and has a width of 4m and k=0.015 terminates with a sill of width 20m and k=0.02. The other dyke (black) has a width of 5m and k=0.02 and extends from a depth of 65m to >2000m. In both instances the strike and dip are N124°E and 63°SW respectively.

3.6 Summary

The reconnaissance ground magnetic survey carried out by the Field School class of 2001 using University of Alberta's portable Proton-Precession Magnetometer to image the postulated characteristic dykes of the study area as stated in Chapter 2. The processed magnetic data in showed the presence of two linear subparallel northwest trending anomalies (Figure 3.7). The southerly anomaly being the predominant one of higher intensity averaging 45nT and the northerly less intense anomaly of average intensity 15nT. However, both anomalies were discontinuous at the central profile line where coincidentally the seismic survey line and the road were located.

Forward modelling of the magnetic data was done using "Potent", a modelling software designed by Geophysical Software Solution for modelling magnetic data. Different 2D models (Figure 3.8-3.10) were obtained using the 4th

profile line east of the seismic line (510m east of the seismic line) at UTM coordinate 442943 east (Figure 3.6(e)). The best model (Figure 3.9) showed two subparallel subvertical dykes where the southernmost one thickened from the bottom to the top and the northernmost anomaly had a regular thickness throughout. The other models Figure 3.8 and 3.9 were also realistic for the study area but was not such a good fit to the observed magnetic data.

Chapter 4

Seismic Data

4.1 Introduction

The seismic method is one of the most important and widely used geophysical techniques because of its high accuracy, high resolution and great penetration. Seismic surveys are predominant in petroleum exploration and are good for stratigraphic investigation.

A seismic survey was conducted in order to attempt to image the characteristic dykes in the study area as shown by past ground magnetic surveys performed by the University of Alberta's Field School in the neighbouring areas; and the aeromagnetic survey carried out in the 1990's by the Geological Survey of Canada (Chapter 3). However, the existence of several relatively small sills and

dykes in the neighbouring Sweet Grass Intrusives (Kjarsgaard), may suggest similar structures in the study area and because of the size and geometry may not show in the processed seismic data.

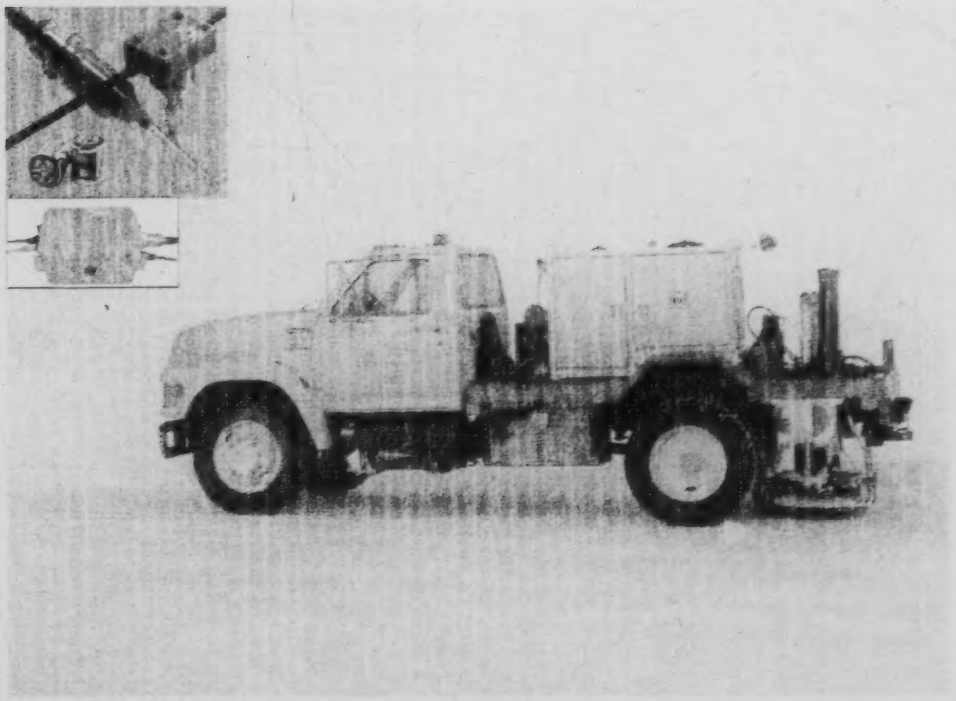

Figure 4.1: The University of Alberta's 2000-6000lbs vibroseis. The top left corner shows a geophone and a geode "box" below.

The seismic data set in the study area was obtained over a two (2) year period by the field class of 2001 and 2002 using the University of Alberta's 2000-6000lb Vibroseis (sometimes referred to as the "minivibe") shown in Figure 4.1. The two (2) data sets (referred to as the Milk River data set) collected in 2001 and 2002 were merged to produce a seismic line with approximately 2.5m common midpoint (see section 4.2.1) coverage in the north-south direction. This merged data set was then processed using basic seismic processing steps (Yilmaz, 1987)

as outlined in Figure 4.2. The software VISTA developed by Seismic Image Software Limited (SIS) was used to process the Milk River data set. The processed data was then modeled using Kingdom Suite interpretational software developed by Seismic Micro Technology. The interpretation was done with the assistance and expertise of Dr. Dean Rokosh using the well, B.A.HB Verdigris (07-26-03-14W4) approximately 12km north east of the seismic survey (Figure 1.2).

4.2 Acquisition

The University of Alberta's minivibe (Figure 4.1), which operates at 10-550Hz was the energy source used to perform the seismic survey in 2001/2002. The resultant signals (traces) from the ground motions in the study area due to the energy source (2000-6000lb minivibe) were recorded via GS-20DM 14Hz OYO single component geophones. Twenty-four geophones are connected to each geode (Figure 4.1). The data was collected in seg2 file format and each seg2 file contained information about all the traces in trace headers recorded from the application of a shot. Each seg2 file is called a shot gather.

In 2001, the data was recorded with 240 geophones at approximately 4m intervals. The 2002 data set was also recorded with 240 geophones at approximately 4m intervals, but continued from the last geophone of the 2001

survey, so the merged data set contained approximately 480 traces. In 2001 the shot spacing was approximately 24m whereas in 2002 the shot spacing was approximately 32m, which resulted in shot spacings with variations between 8-24m in the merged data set. The 2002 data set started with the first shot at the same position as the first shot of the 2001 survey. In both cases the receivers (geophones) remained stationary and the shot source moved along the receiver line with all the geophones recording the reflected seismic signals.

Additionally, the GPS x (East-West direction), y (North-South direction) and z (elevation) positions (according to the Universal Transverse Mercator (UTM) Grid System) for the receivers and shot points were obtained by the University of Alberta's Trimble 4600 LS Differential GPS unit.

4.3 Processing

4.3.1 Methodology

The Milk River reflection seismic data set was processed using VISTA and the processing flow (Yilmaz, 1987) shown in Figure 4.2. As a prerequisite for the processing of the data with VISTA the data were converted from seg2 to segy file format. The GPS x, y, and z positions of the shots and receivers obtained using

the University of Alberta's Trimble GPS unit were then integrated into the VISTA headers thus creating the geometry of the seismic survey in VISTA.

Each segy file contains a shot gather and the traces in a shot gather are caused by reflections of wave energy at different layer interfaces in the earth. Traces within the shot gathers can be resorted so that seismic energy reflected from a common point may be grouped together. In reality, the seismic energy is not reflected from exactly a common point but from approximately a common point, which may be called a "common area". These groups are called common midpoint (CMP) gathers. Consequently, positions of the midpoints were calculated for the survey and CMP bin spacings of 4m in the NS and 2m in the EW directions were created. CMP bins are used because CMPs do not represent seismic energy reflected from exactly a common point but from a common area as described above. Each bin was assigned a CMP number and traces with common midpoints within a bin were assigned this CMP number.

Automatic gain control (AGC) scaling was used to correct for amplitude loss with time since the amplitude of the raw data decreased with time and consequently, obtain an enhanced display of the data. Amplitude loss is due to the loss of energy and this loss of energy is caused by spherical divergence, reflection and transmission at reflectors (or boundaries), absorption and scattering. Spherical divergence is due to the area of a wavefront increasing with time. Incident energy is divided at a boundary since energy is reflected, refracted and transmitted at the boundary. Absorption is the loss of energy due to friction in the earth and scattering is the loss of energy at an obstacle. The AGC calculates the average

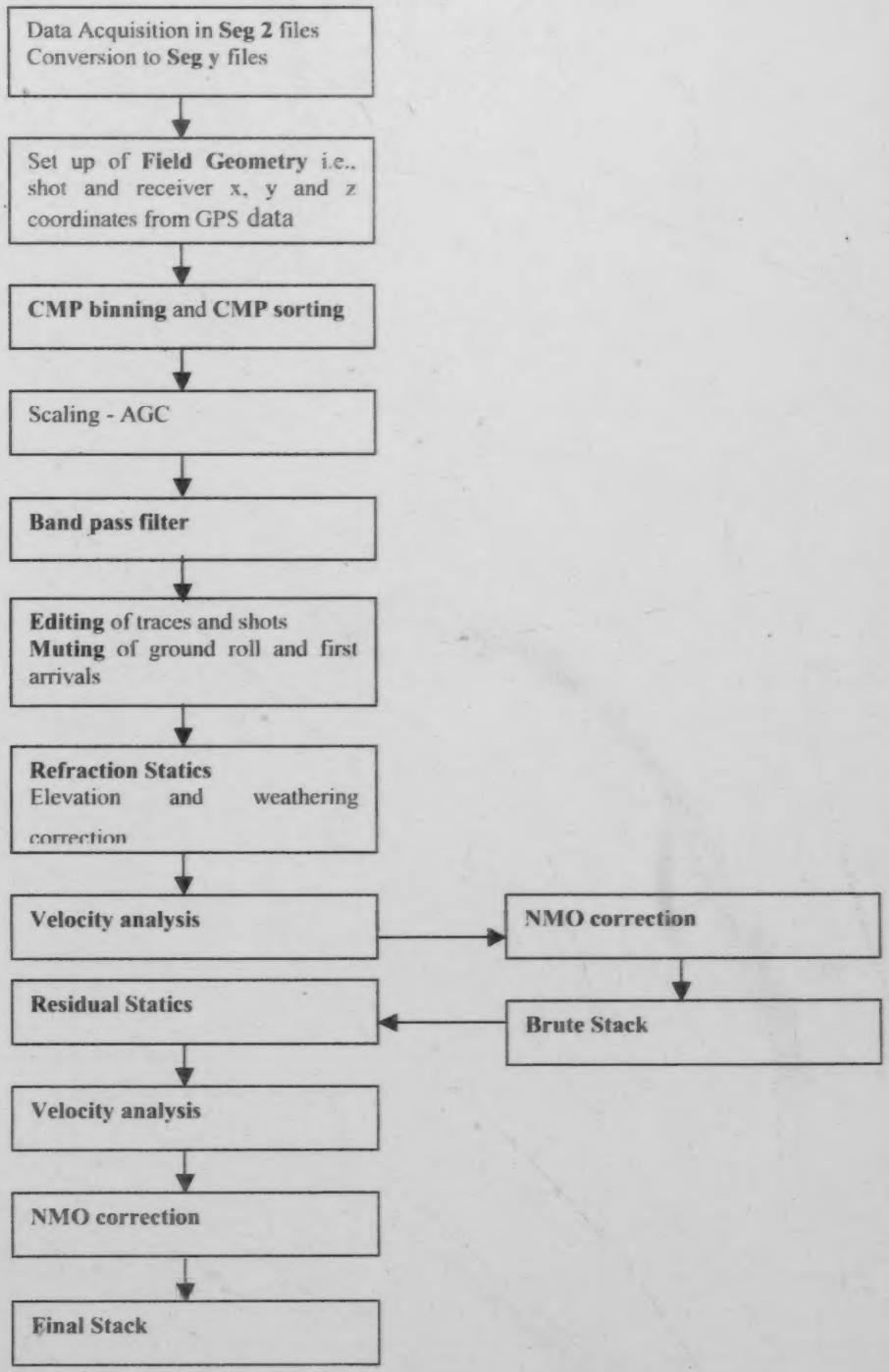
Data Acquisition in Seg 2 files
Conversion to Seg y files
Set up of Field Geometry i.e., shot and receiver x, y and z coordinates from GPS data
CMP binning and CMP sorting
Scaling - AGC
Band pass filter
Editing of traces and shots
Muting of ground roll and first arrivals
Refraction Statics
Elevation and weathering correction
Velocity analysis
NMO correction
Residual Statics
Brute Stack
Velocity analysis
NMO correction
Final Stack

Figure 4.2: Processing flow for the Milk River reflection seismic data set. Modified from Yilmaz, 1987

absolute amplitude of all the samples in a trace within a moving AGC window and the sample at the centre of the window is then multiplied by scaling factor/average. The window moves down one sample and starts again. This process continues to the end of the trace and is done on a trace-by-trace basis. In the Milk River data set a window length of 500ms and a scaling factor of 1 was used.

A band pass filter was applied to all shot gathers to remove coherent and ambient noise and as a result improve the signal to noise ratio. Frequencies below 15Hz and beyond 70Hz were removed. Figure 4.3 shows a raw shot (shot 101 from the Milk River data set) and the raw shot after applying an AGC scaling and a band pass filter to the Milk River data set.

The shots and traces of the Milk River data set were then edited. Poorly recorded shots and traces were killed (setting the amplitude of the entire trace to zero). Ground roll (low frequency noise) and first arrivals were muted (Figure 4.3 and Figure 4.5). Muting sets the amplitude of the selected contaminated portions of traces to zero.

Refraction static corrections were then applied to the data set in order to correct for variations in the elevation of the shot points and receivers as well as the near surface low velocity-weathering layer. These variations affect travel times and time shifts are used to set the shot points and receivers to a common datum surface. The assumption is that the conditions are uniform and there is no low velocity layer below the datum surface (Telford et. al., 1990). The datum for the Milk River data set was 930m.

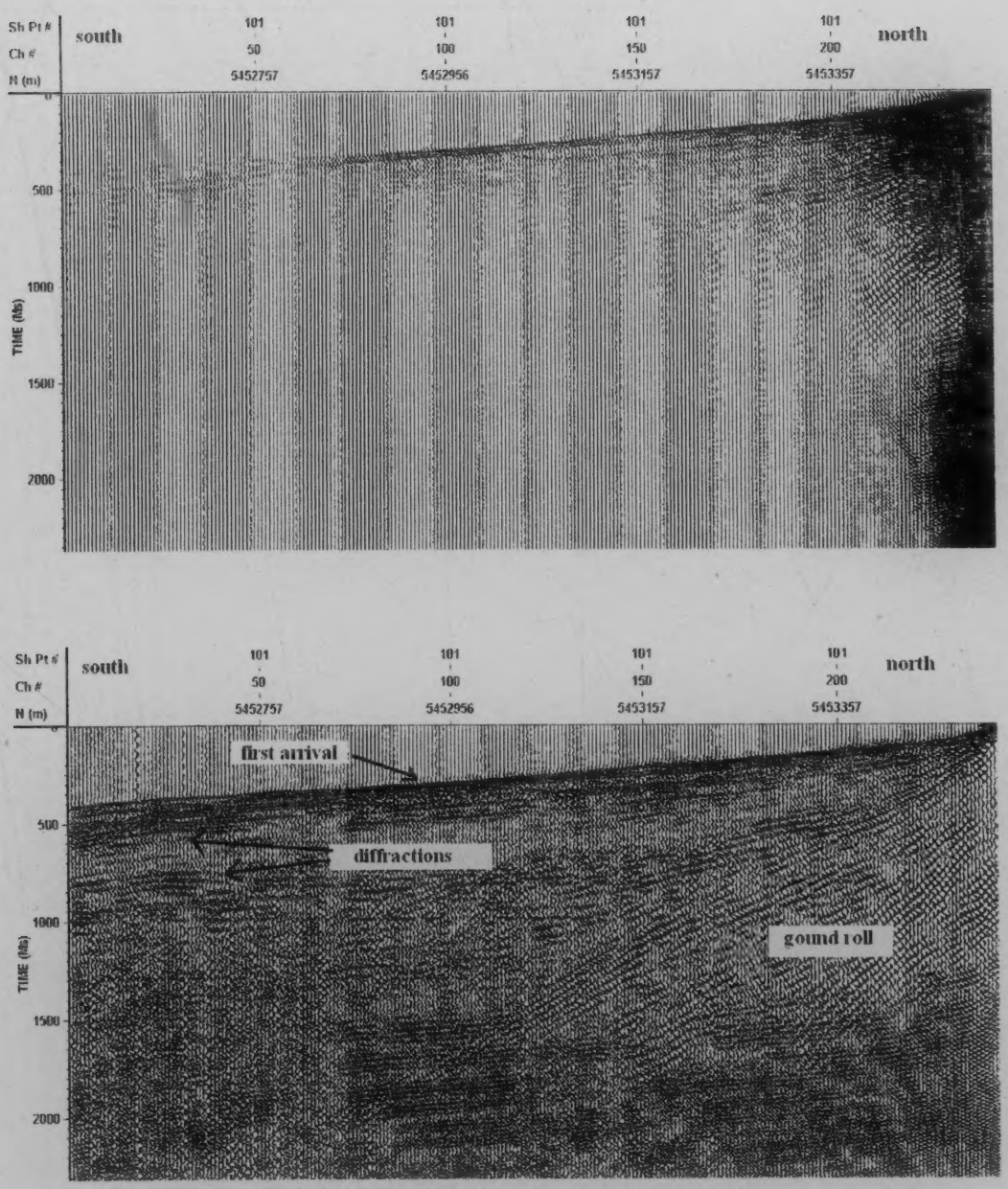

Figure 4.3: Shot gather for the northernmost shot point (shot 101 from the Milk River data set). Top horizontal axis is Shot point # (Sh Pt #), channel number (Ch #) – scale 3cm=50Ch and northings (N) in metres – scale 3cm=200m. Vertical axis is time in milliseconds – 1cm=300ms. Top figure shows a raw shot (Shot 101 from the Milk River data set) and bottom figure shows the raw shot after applying an AGC scaling and a band pass filter.

CMP gathers contain traces from the same point in a reflector (as mentioned earlier), but the travel paths are different and these travel paths cause different travel times. Therefore, a reflector appears as a hyperbolic event in a CMP gather. Velocity analysis finds velocities that can flatten these hyperbolic events by using two (2) common tools - semblance and constant velocity stack (CVS). Semblance is a measure of the coherency of the signal for a range of velocities. CVS shows different panels of several stacked CMPs after normal move out (NMO) correction where a constant velocity is applied to each panel over the entire time range. The NMO correction essentially removes the time delay from source to receiver for the non-zero offset traces in a CMP gather. Velocities were picked in the merged data set for ten (10) successive CMPs and interpolated across all the CMPs, thus producing a velocity function.

This velocity function was used to apply the NMO correction to all the CMP gathers over the entire time range. The velocity function flattened the hyperbolic events and after the traces within a CMP gather were summed. This summation of traces in a CMP gather is called stacking and stacking tends to increase the signal to noise ratio. Stacked traces from each CMP ensemble are displayed next to each other to produce a "brute stack" (or preliminary stack). Each stacked trace from a CMP gather represents the reflection from the same point in an event. The residual statics was then calculated and applied to the data. A velocity function was again obtained from the "static corrected" data and this new velocity function was used for NMO correction and a final stack obtained.

4.3.2 Results

The processed seismic data shown in Figure 4.4 was obtained using the process flow from Figure 4.2 (Yilmaz, 1987) and VISTA software package. The top horizontal axis is the common midpoint number (CMP #) and northings (N) in metres. The vertical axis is two-way travel- time in milliseconds. The good data between 200ms and 1400ms are illustrated. Strong continuous reflections are seen at 600 and 760ms. Weaker discontinuous reflections are observed at 660, 700, 780, 820, 870 and 920 ms. The bottom graph (red curve) represents the processed magnetic profile along the seismic line, that is, magnetic field (nT) versus northings (m).

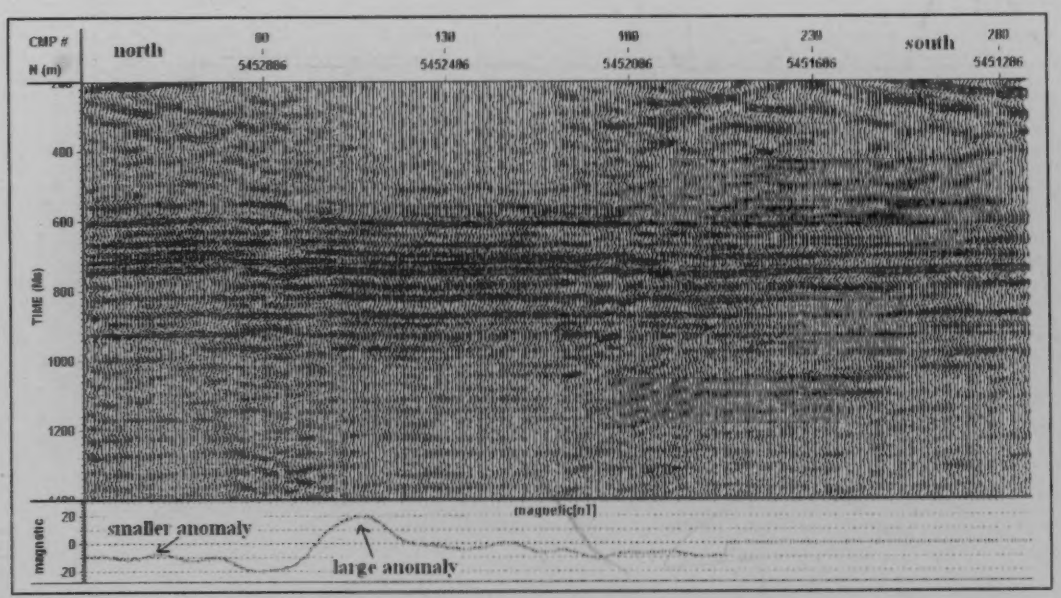

Figure 4.4: Processed seismic data in VISTA using process flow from Figure 4.2. Top horizontal axis is common midpoint number (CMP #) – scale 3cm=50CMP and northings (N) in metres – scale 3cm=400m. Vertical axis is time in milliseconds – 1cm=200ms. Bottom graph (red) shows the magnetic profile along the seismic line, magnetic field (nT) vs. N (m) - Vertical scale 1cm=40nT and horizontal scale 3cm=400m

In Chapter 3 it was mentioned that the shape of the profile along the seismic line was different from those profiles west and east of it. The image of the magnetic survey area (Figure 3.7) showed two (2) linear subparallel northwest trending anomalies, that were discontinuous where the seismic line intersected the anomalies, which was coincidentally along the road. These two anomalies were discontinuous meant that their magnetic intensities were less where the "seismic line" magnetic profile line traversed the anomalies relative to the profiles to the east and west of the magnetic profile along the seismic line. Assuming the anomalies were continuous across the road, by interpolation the smaller anomaly would be expected at approximately 5453100m (corresponding to CMP# 52) and the larger anomaly expected to be around 5452700m (corresponding to CMP# 100). However, both anomalies did not appear in the processed seismic data. This may not be completely unexpected since vertical features cannot be imaged using standard reflection seismic methods.

Figure 4.5 shows a shot gather for the northernmost shot point (shot point 101). The top horizontal axis is shot point number (Sh Pt), channel number (Ch #) and northings (N) in metres. The vertical axis is two-way travel-time in milliseconds. This shot gather shows the ground roll and first arrivals that were muted, as mentioned in the previous section, but most importantly the diffractions are illustrated. The bottom graph (red) shows the magnetic profile along the seismic line, magnetic field (nT) vs. northings (m). The location of the large anomaly corresponds to that of the seismic diffractions in the shot gather. Diffractions are the scattering of seismic energy in a radial fashion and occur at

abrupt discontinuities in interfaces, or structures whose radius of curvature is shorter than the wavelength of the incident waves (Kearey and Brooks, 1991). Common sources of diffractions are edges of faulted layers and isolated structures such as a dyke in this instance. The expected smaller anomaly does not show in this shot gather and this could be due to the proximity of the energy source (northernmost point) and the associated low frequency, high amplitude ground roll that could obscure any diffractions.

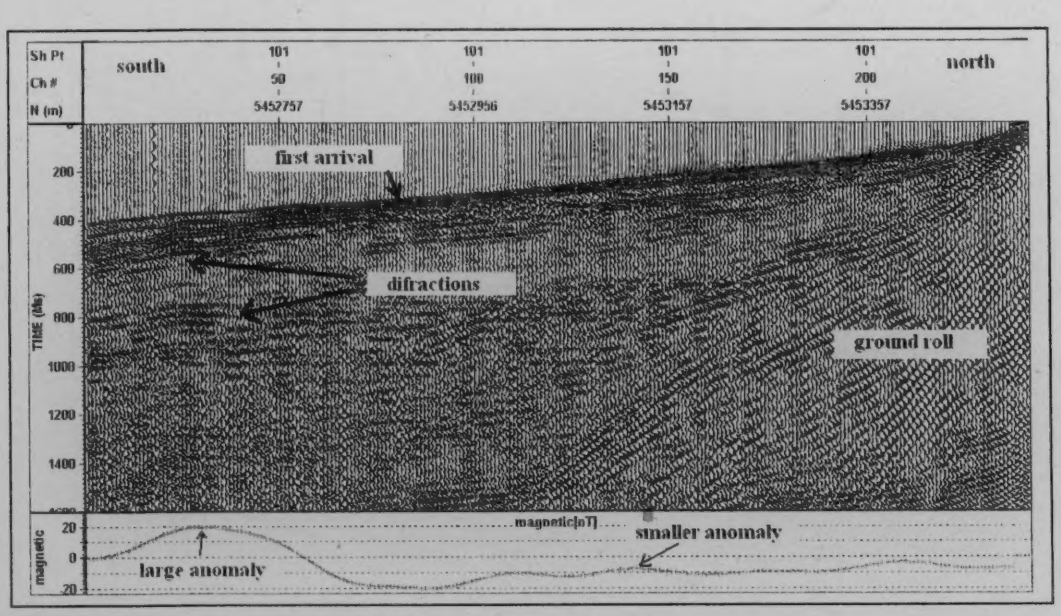

Figure 4.5: Shot gather for the northernmost shot point (shot 101 from the Milk River data set). Top horizontal axis is Shot point # (Sh Pt), channel number (Ch #) – scale 3cm=50Ch and northings (N) in metres – scale 3cm=200m. Vertical axis is time in milliseconds – 1cm=250ms. Bottom graph (red) shows the magnetic profile along the seismic line, magnetic field (nT) vs. N (m) - Vertical scale 1cm=40nT and horizontal scale 3cm=400m

Consequently, shot point 401 approximately 1.2km south of shot point 101 was examined in order to eliminate the proximity factor and hence the concealing

effect of ground roll. Figure 4.6 illustrates the shot gather for shot point 401. The top horizontal axis is shot point (Sh. Pt.), channel number (Ch #) and nothings (N) in metres. The vertical axis is two way travel-time in milliseconds and the bottom graph (red) shows the magnetic profile along the seismic line, magnetic field (nT) vs. N (m). Again diffractions correspond to the large anomaly but diffractions representing the expected small anomaly do not appear to exist.

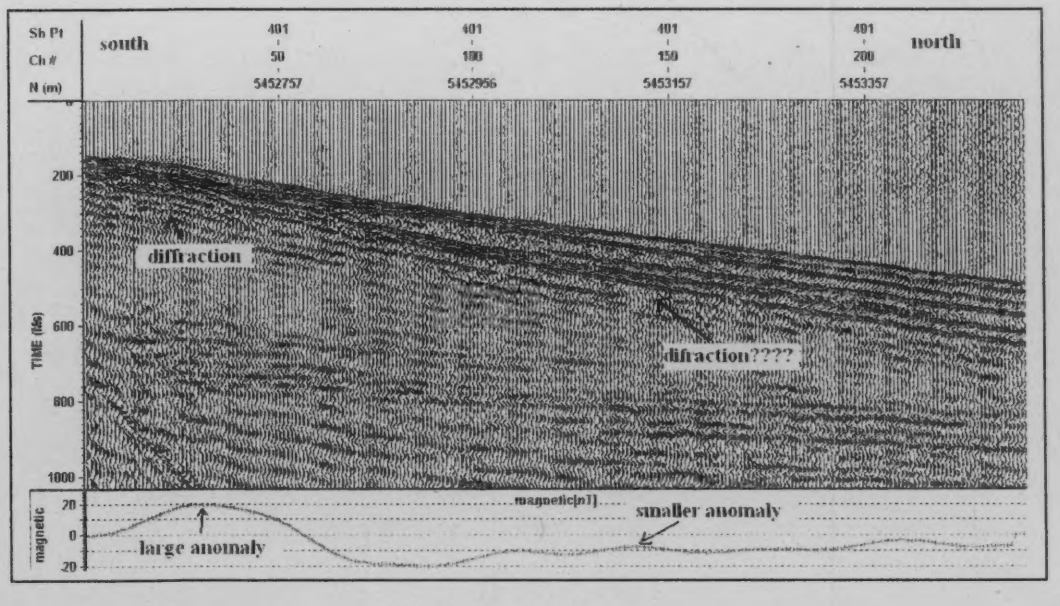

Figure 4.6: Shot gather for the shot point 401, approximately 1.2km south of northernmost shot point. Top horizontal axis is Shot point (Sh Pt), channel number (Ch #) – scale 3cm=50Ch and northings (N) in metres – scale 3cm=200m. Vertical axis is time in milliseconds – 1cm=200ms. Bottom graph (red) shows the magnetic profile along the seismic line, magnetic field (nT) vs. N (m) - Vertical scale 1cm=40nT and horizontal scale 3cm=400m

4.4 Seismic Modelling and Interpretation

The well B.A.HB Verdigris (07-26-03-14W4) located approximately 12km north east of the seismic survey (Figure 1.2) was used to model and interpret the data. The sonic log data, which is a measure of slowness with depth, was converted to velocity versus time. Figure 4.7 shows the time (s) versus depth (m) curve obtained from the well B.A.HB Verdigris (07-26-03-14W4). The formation tops; 2nd White Specks, Base of Fish Scales, Mannville, Sunburst, Reirdon, Livingstone, Banff, Exshaw, Stettler, Cooking Lake, Beaver Hill Lake, Deadwood, Pika, Eldon, Earlie, Cathedral and Mount Whyte encountered at this well were shown in the time (s) versus depth (m) curve and were discussed in Chapter 2.

The time series obtained from the well B.A.HB Verdigris (07-26-03-14W4) and the Milk River data set processed in VISTA were imported into Kingdom Suite. A synthetic seismogram was then calculated by convolving a wavelet extracted from the processed Milk River data with the time series obtained from the well data. This synthetic seismogram together with the stratigraphic chart (Figure 2.7) was then used to interpret the seismic data (Figure 4.7). This interpretation was done with the assistance of Dr. Dean Rokosh.

In the processed seismic section (Figure 4.3 and Figure 4.7) it was difficult to determine whether any structure such as a dyke was present. However, some formation tops found at the well B.A.HB Verdigris (07-26-03-14W4) were

identifiable; namely the Mannville (MNVL) at ~0.65 secs, Rierdon/Livingstone (R/Liv.) at ~0.74 secs, Stettler (Stet.) at ~0.88 secs, Beaver Hill Lake (BHL) at ~1 secs, Deadwood (DDWD) at ~1.04 secs, Pika at ~1.09 secs and the Precambrian basement (PreC.) at ~1.18 secs.

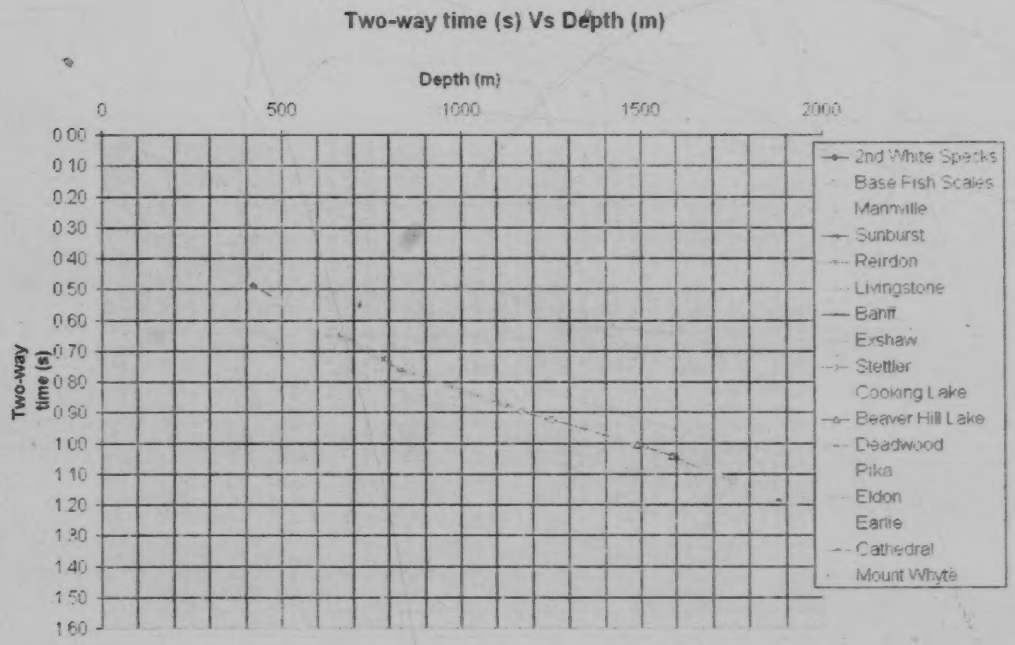

Figure 4.7: Time (s) versus depth (m) curve obtained from the well B.A.HB Verdigris (07-26-03-14W4). The formation tops encountered at this well; 2nd White Specks, Base of Fish Scales, Mannville, Sunburst, Reirdon, Livingstone, Banff, Exshaw, Stettler, Cooking Lake, Beaver Hill Lake, Deadwood, Pika, Eldon, Earlie, Cathedral and Mount Whyte are shown.

The major unconformities as outlined in Chapter 2 are shown in Figure 4.8 also. These unconformities are at Rierdon/Livingstone (~0.74 secs), Deadwood (~1.04 secs) and at the top of the Precambrian (~1.18 secs).

The depths corresponding to the two way travel times of the interpreted formation tops were obtained using the time depth curve in Figure 4.7 and are show in Table 4.1. The Lower Cretaceous Mannville Group was at a depth of approximately 664m and generally contains interbedded marine and non-marine shale, siltstone and fine-grained sandstone. A minor unconformity (i.e. very little rocks have been eroded) occurs at the top of the Mannville Group but is not shown in Figure 4.8.

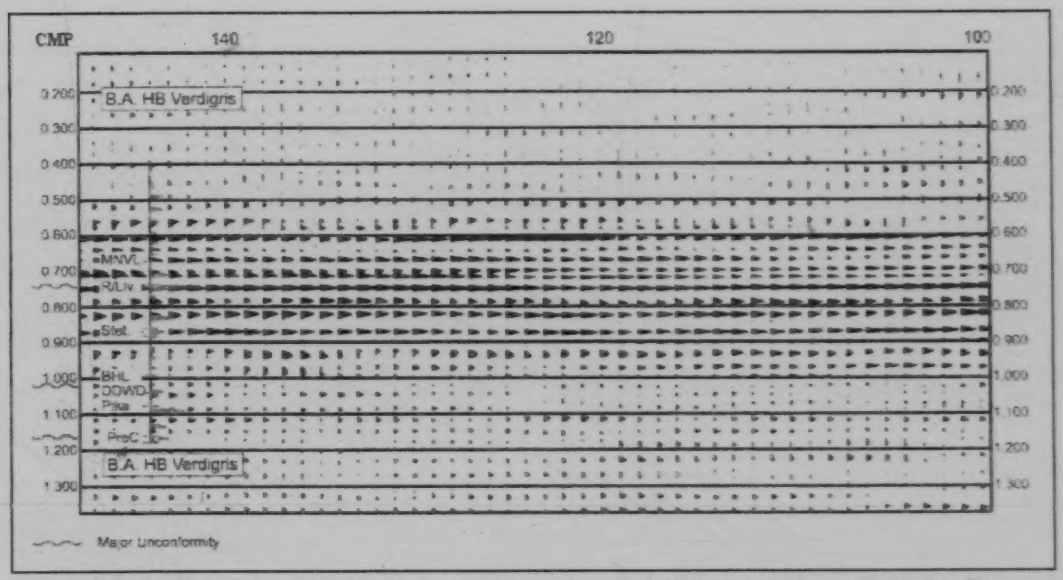

Figure 4.8: The interpreted seismic section using B.A.HB Verdigris well (red). Top horizontal axis is common midpoint number (CMP) – scale 3cm=20CMP. Vertical axis is time in seconds – 1cm=0.3s. Formation tops such as the Mannville (MNVL), Rierdon/Livingstone (R/Liv.), Stettler (Stet.), Beaver Hill Lake (BHL), Deadwood (DDWD), Pika and the Precambrian basement (PreC.) are shown.

The Rierdon Formation is of Mississippian (Carboniferous) age and it contains shales and is partly calcareous with minor limestone interbeds. The Rierdon Formation has an unconformity above it but conformably rests on the

Livingstone Formation. The Lower Carboniferous (Mississippian) Livingstone Formation comprises carbonates, mainly clean limestone and dolostone. They were both at a depth of approximately 800m.

Formation Tops	2 way travel time/secs	Depth/m
Mannville	0.65	664
Rierdon/Livingstone	0.74	800
Stettler	0.88	1168
Beaver Hill Lake	1.00	1489
Deadwood	1.04	1599
Pika	1.09	1658
Precambrian	1.18	1920

Table 4.1: Interpreted formation tops and their 2 way travel time and depth.

The Upper Devonian Stettler Formation is comprised mostly of carbonates and anhydrites and occurs at a depth of approximately 1168m.

The Beaverhill Lake Group lays unconformably on the Cambrian Deadwood Formation. It is the start of the Devonian Period and its top is at a depth of approximately 1489m. The Beaverhill Lake Group contains open marine carbonates that covers most of the WCSB.

This Deadwood formation is Late Cambrian in age, and consists of interbedded shales and siltstones. It conformably overlies the Pika Formation at a depth of approximately 1599m.

The Pika Formation comprises mostly limestones and dolomites. It is usually used as a marker bed to locate the overlying Deadwood formation. This Formation is of late Middle Cambrian in age and occurs at a depth of 1658m.

Precambrian crystalline basement is at a depth of 1920m and consists of Archean and Proterozoic intrusive and metamorphic rocks.

4.5 Seismic Resolution Issues

Vertical and horizontal resolution may have played a role in the failure to image the dykes and some of the other lithological boundaries. The extent to how close two points can be and yet be distinguishable defines resolution. Both vertical and horizontal resolutions are controlled by frequency.

Vertical resolution is a measure of the ability to identify reflectors that are closely spaced and it is determined by the wavelength of traces in a seismic section. The maximum vertical resolution possible is usually between one quarter and one eight of the dominant wavelength of the trace in a seismic section (Kearey and Brooks, 1991). In the Milk River seismic data set, the dominant frequency is 30Hz and the average velocity of the good data (200-1400ms) is 4000m/s. The seismic wavelength is ~133m and was obtained using the following equation:

$$v = f\lambda \qquad 4.1$$

where v = velocity (m/s)

f = frequency (Hz)

λ = wavelength (m)

Therefore the thickness of a resolvable feature must be greater than ~33m.

Lateral resolution relates to how close two reflecting points can be situated horizontally and yet be acknowledged as two separate points. It is often taken as the width of the first Fresnel zone. The Fresnel zone is that part of a reflector where reflected energy can reach a detector within one half wavelength of the first reflected energy. The first Fresnel zone is circular and successive Fresnel zones are annular zones of larger radii. For an interface to be observed it must be at least as wide as the first Fresnel zone. Horizontal resolution like vertical resolution is dependant on wavelength in addition to depth. The width of the Fresnel zone is given:

$$w = (2z\lambda)^{1/2} \qquad 4.2$$

where w = width

z = depth (m)

λ = wavelength (m)

Then, the lateral resolution reduces from ~230m at 200ms to ~730m at 1100ms.

4.6 Summary

The reflection seismic survey was performed within a two (2) year period by the field class of 2001 and 2002 using the University of Alberta's 2000-6000lb Vibroseis in order to attempt to image the characteristic dykes of the study area. The basic seismic processing done on the Milk River data set does not seem to image the dykes cutting the sedimentary layers. However, the processed Milk River data set does show some of the reflecting lithologic boundaries. The processed magnetic data showed two parallel anomalies that were discontinuous where they intersected the seismic survey line. The raw shots of the seismic data illustrated that; there were diffractions at the larger anomaly but no diffractions where the small anomaly would be expected if the anomalies were continuous. Although the intensity of the large anomaly was small (~20nT) compared to the other profiles east and west it did show as diffractions in a raw shot.

These reflection boundaries (formation tops) observed in the Milk River data set were interpreted using the tie well B.A.HB Verdigris (07-26-03-14W4) 1.2km located northwest of the study area. This tie well was also used for the transformation of these interpreted formation tops from the time to the depth domain. The interpreted Formation tops are as follows: Mannville (MNVL) at ~0.65 secs (664m), Rierdon/Livingstone (R/Liv.) at ~0.74 secs (800m), Stettler (Stet.) at ~0.88 secs (1168m), Beaver Hill Lake (BHL) at ~1 secs (1489m),

Deadwood (DDWD) at ~1.04 secs (1599m), Pika at ~1.09 secs (1658m) and the Precambrian basement (PreC.) at ~1.18 secs (1920m).

Chapter 5

Discussion and Conclusion

The purpose of the geophysical surveys, performed by the field school classes of 2001 and 2002 of the University of Alberta was to attempt to image and study the dykes postulated to exist beneath the surface in the Milk River area. The existence of these potential dykes were supported by past aeromagnetic surveys done in the fall of 1992 by the GSC in south Alberta and analyzed by Ross et. al., 1996 (Chapter 3); as well as ground magnetic surveys carried out by the field school class of the University of Alberta prior to this study in the vicinity of the study area (Figure 2.1). Furthermore, the geological overview provided in chapter 2 permitted some correlations to be made between the Sweetgrass hills and the SGI (Kjarsgaard, 1994). Subsequently it was hypothesized that the SGI was analogous to the study area due to their proximity.

This thesis provided an overview of the acquisition, processing and modelling and interpretation of magnetic (Chapter 3) and seismic (Chapter 4) data collected by the Field School classes of the University of Alberta near the Milk River area, southern Alberta. This was accompanied by a brief geological overview of Alberta and a more detailed geological study of the areas (Chapter 2) where the magnetic and seismic surveys were performed.

Whole rock and trace element chemistry, mineralogy and mineral chemistry have provided evidence that the rocks in SGI are mainly minettes and that these minettes are similar to those found in the SGH of the Montana alkaline province (Kjarsgaard 1994). Geochemical data for these minettes in the Milk River area indicated that they are similar to the mantle derived rocks from the Archean Wyoming craton (Buhlmann et. al., 2000) and by extension possibly the hypabyssal intrusive rocks in the study area originated from the mantle (>100km). Therefore the rocks in the study area are classified as mantle derived minettes. The SGI are essentially shallow mafic potassic-rich magmatic rocks of Eocene (49-53 Ma) age (Kjarsgaard, 1997 and Marvin et. al., 1980). The anomalies in the study area by extension could also be hypabyssal intrusives of the Eocene age.

The magnetic data was collected in August 2001 using the University of Alberta's GSM-19 Overhauser Proton Precession Ground Magnetometer over an area of approximately 1.6km by 1.3km in the north-south and west-east directions respectively. The processed data illustrated an image of two linear subparallel northwest trending anomalies. The linearity of the magnetic anomalies may

suggest that they were dykes formed by extension and formation of dilatational fractures that are filled with minette magma (Ross et. al., 1996).

These anomalies appeared discontinuous along the magnetic line, which was coincidentally along the road and the seismic line also. Forward 2D modelling of the observed magnetic data from the 4th profile line east of the seismic line (510m east of the seismic line) using "Potent" showed the best fit model was two subparallel (strike ~ N124°E) subvertical (dip ~ 63°SW) dykes. The southernmost dyke of higher magnetic intensity thickened from 4m at a depth greater than 2000m to a width of to 20m at an 85m depth at the top whereas the other northernmost dyke had a regular width of 5m and extended from 65m to beyond 2000m depths. The 4th profile line was not perpendicular to the observed anomalies and this can result in the anomalies having an apparently longer wavelength than in reality (Kirton and Donato, 1985). Based on the analogy with the outcrops in the SGI (Chapter 2) the abovementioned model parameters and resultant model is very feasible. The magnetic susceptibility values used were determined using the range of values obtained from rocks in the SGI area by Kjarsgaard, 1994 and Ross et. al., 1996. The model showed the dyke originated from beyond 2km in depth and this is consistent with models presented by Ross et. al., 1996 of the neighbouring areas.

The University of Alberta geophysics field class conducted a reflection seismic survey over a two (2) year period using its 2000-6000lb Vibroseis. The two data sets obtained in 2001 and 2002 were merged (called the Milk River data set) and processed using VISTA, in order to attempt to image the characteristic

dykes of the study area. The processed Milk River data set data set does not seem to image the dykes cutting the sedimentary layers. However, the processed Milk River data set does show some of the reflecting boundaries. These reflection boundaries are continuous along the seismic line and therefore show a good image after CMP stacking. CMP stacking tends to enhance such continuous features but somehow suppresses localized features such as a subvertical dyke. Since the dykes were modeled in Chapter 3 as subvertical and thin they were not expected to appear in the processed seismic data because there is limited seismic lateral and vertical resolution for such small features

The reflection boundaries (formation tops) observed in the Milk River data set were interpreted as the Mannville (MNVL) at ~0.65 secs (664m), Rierdon/Livingstone (R/Liv.) at ~0.74 secs (800m), Stettler (Stet.) at ~0.88 secs (1168m), Beaver Hill Lake (BHL) at ~1 secs (1489m), Deadwood (DDWD) at ~1.04 secs (1599m), Pika at ~1.09 secs (1658m) and the Precambrian basement (PreC.) at ~1.18 secs (1920m). This interpretation utilized the tie well B.A.HB Verdigris (07-26-03-14W4) located 12km northwest of the study area and which was also used for the transformation of these interpreted formation tops from the time to the depth domain.

The processed magnetic data (Chapter 3) showed two linear subparallel northwest trending anomalies that were discontinuous where the magnetic profile line along the seismic survey line intersected these anomalies. The raw shots of the seismic data illustrated that; there were diffractions at the larger anomaly but no diffractions where the small anomaly would be expected if the anomalies were

continuous. Although the intensity of the large anomaly was small (~20nT) relative to the profiles east and west, it did show as diffractions in a raw shot traversing the anomalies. The magnetic discontinuity along the seismic line on the road was thought to be due to some disguising effect of the material laid on the road thus obtaining false magnetic readings. However, the fact that the larger anomaly showed as diffractions in a shot traversing both the anomalies meant that the larger existed and the smaller anomaly was either so insignificant it did not result in diffractions or the diffracted waves from it were overwhelmed by those corresponding to the larger anomaly.

Bibliography

Bates, R.L. and Jackson, J.A., 1983 (ed.), Dictionary of Geological Terms, American Geological Institute, New York.

Buhlmann, A. L., Cavell, P., Burwash, B. A., Creaser, R. A., and Luth, R. W., 2000, Minette bodies and cognate mica-clinopyroxenite xenoliths from the Milk River area, southern Alberta: records of a complex history of the northernmost part of the Archean Wyoming craton. Canadian Journal of Earth Sciences, **37**: 1629-1650.

Burwash, R.A. and Cavell, P.A., 1992, Xenoliths in ultrapotassic rocks of the Sweetgrass Arch, Alberta: evidence of a Mid-Proterozoic mantle metasomatism; Rocky Mountain section, Geological Society of America, Program with abstracts, v. 24, no. 6, p. 5.

Davis, W. J. and Kjarsgaard, B.A., 1994, A Rb-Sr phlogopite-whole rock isochron age for olivine minette from the Milk River area, southern Alberta, Radiogenic Age and Isotropic Studies: Report 8. Geological Survey of Canada, Current Research 1994-F, p. 11-14.

Dawson, G.M., 1884, Geological Survey of Canada, Report of Progress1982-83-84 part C, p. 16-17 and 45-47

Fowler, C.M.R., 1990, The Solid Earth: An introduction to Global Geophysics, Cambridge Press, United Kingdom.

Grant, F.S. and West, G.F., 1965, Interpretation Theory in Applied Geophysics. McGraw Hill, New York.

Kirton, S.R. and Donato, J.A., 1985, Some buried Tertiary dykes of Britain and surrounding waters deduced by magnetic modelling and seismic reflection methods, J. geol. Soc. London, Vol. 142, p. 1047-1057.

Kearey, P. and Brooks, M., 1991, An Introduction to Geophysical Exploration, Blackwell Science, United Kingdom.

Kemp, J.F. and Billingsley, P., 1921, Sweet Grass Hills, Montana. Geological Society of America Bulletin, v. 32, p. 437-478.

Kjarsgaard, B.A., 1994, Potassic magmatism in the Milk River area, southern Alberta: petrology and economic potential. *In* Current Research, 1994-B Geological Survey of Canada, p. 59-68.

Kjarsgaard, B.A., and Davis, W.J., 1994, Eocene magmatism in the Sweet Grass Hills and its tectonic significance. *In* Lithoprobe Alberta Basement Transects Workshops, February 14-15, 1994, G.M. Ross (ed.). Publication no. 37, Lithoprobe Secretariat University of British Columbia, p. 234- 237.

Kjarsgaard, B.A., 1997, Diamonds in Alberta: studies of potential host rocks of deep-seated origin and applications of indicator mineral exploration techniques. Geological Survey of Canada, Bulletin 500, p. 185-207

McQueen, R. W., 1994, Geological Survey of Canada Canada-Alberta Partnership on Minerals: Geological Survey of Canada Projects and Progress.

Marvin, R.F., Hearn, B.C.J., Mehnert, H.H., Naeser, C.W., Zartman, R.E. and Lindsey, D.A., 1980, Late Cretaceous-Paleocene-Eocene igneous activity in north central Montana. Isochron/West, 29: 5-25.

Meyboon, P., 1960, Geology and groundwater resources of the Milk River Sandstone in Southern Alberta, Research Council of Alberta, Memoir 2

Mossop, G. D., and Shetsen, I. (compilers), 1994, Geological Atlas of the Western Canadian Sedimentary Basin. Canadian Society of Petroleum Geologists and Alberta Research Council.

Porter, J. W., Price, R. A., and McCrossan, R. G., 1982, The Western Canadian Sedimentary Basin. *In* The Evolution of Sedimentary Basins. Proceedings of a Royal Society Discussion Meeting. Philosophical Transactions of he Royal Society of London, series A, v. 305, Royal Society, London, p. 169-192.

Ricketts, B. D. (ed), 1989, Western Canadian Sedimentary Basin: a Case History, Canadian Society of Petroleum Geologists, Calgary.

Ross, G.M., Mariano, J., and Dumont R., 1994, Was Eocene magmatism widespread in the subsurface of southern Alberta? Evidence from new aeromagnetic anomaly data. *In* Lithoprobe Alberta Basement Transects Workshops, February 14-15, 1994, G.M. Ross (ed.), Lithoprobe Report no. 37, Lithoprobe Secretariat, University of British Columbia, p. 240-249.

Ross, G.M., Mariano, J., Dumont, R., Kjarsgaard, B.A., and Teskey, D., 1996, Was Eocene magmatism widespread in the subsurface of southern Alberta? Evidence from new aeromagnetic anomaly data. Geological Survey of Canada, Bulletin 500, p. 235-246.

Ross, G.M., Parrish, R.R., Villeneuve, M.E. and Bowring, S.A., 1991, Geophysics and geochronology of the crystalline basement of the Alberta Basin, western Canada. Canadian Journal of Earth Sciences, v. 28, p. 512-522.

Russell, L.S. and Landes, R. W., 1940, Geology of the southern Alberta plains. Geologic Survey of Canada, Memoir 221.

Schwarz, E.J., Hood, P.J. and Teskey, D.J., 1987, Magnetic expression of Canadian diabase dykes and downward modelling. *In* Mafic dyke swarms, H.C. Halls and W.F. Fahrig (eds.). Geological Association of Canada, Special Paper 34, p. 153-162.

Sheriff, R.E., 1991, Encyclopedic Dictionary of Exploration Geophysicists, SEG Publications.

Telford, W.M., Geldart, L.P. and Sheriff, R.E., 1990, Applied geophysics, Cambridge Press, United Kingdom.

West, G.F. and Ernst, R.E., 1991, Evidence of aeromagnetics on the configuration of Matachewan dykes and the tectonic evolution of the Kapuskasing Structural Zone, Ontario, Canada. Canadian Journal of Earth Sciences, v. 28, p.1797-1811.

Weed, W.H., and Pirsson, L.V., 1895, On the igneous rocks of the Sweet Grass Hills, Montana, American Journal of Science, Third Series, v. L, no. 298, p. 309-313.

Villeneuve, M.E., Ross, G.M., Theriault, R.J., Miles, W., Parrish, R.R. and Broome, J., 1993, Tectonic subdivision and U-Pb geochronology of the crystalline basement of the Alberta basin, western Canada. Geological Survey of Canada, Bulletin 447, p. 86

Yilmaz, O., 1987, Seismic data processing, SEG Publications.